

Efficient quantum algorithms for testing symmetries of open quantum systems

Rahul Bandyopadhyay* Alex H. Rubin[†]* Marina Radulaski*
Mark M. Wilde[‡]

November 20, 2023

Abstract

Symmetry is an important and unifying notion in many areas of physics. In quantum mechanics, it is possible to eliminate degrees of freedom from a system by leveraging symmetry to identify the possible physical transitions. This allows us to simplify calculations and characterize potentially complicated dynamics of the system with relative ease. Previous works have focused on devising quantum algorithms to ascertain symmetries by means of fidelity-based symmetry measures. In our present work, we develop alternative symmetry testing quantum algorithms that are efficiently implementable on quantum computers. Our approach estimates asymmetry measures based on the Hilbert–Schmidt distance, which is significantly easier, in a computational sense, than using fidelity as a metric. The method is derived to measure symmetries of states, channels, Lindbladians, and measurements. We apply this method to a number of scenarios involving open quantum systems, including the amplitude damping channel and a spin chain, and we test for symmetries within and outside the finite symmetry group of the Hamiltonian and Lindblad operators.

We dedicate our paper to the memory of Göran Lindblad (July 9, 1940–November 30, 2022), whose profound contributions to quantum information science, in the form of the Lindblad master equation [47] and the data-processing inequality for quantum relative entropy [46], will never be forgotten.

*Department of Electrical and Computer Engineering, University of California, Davis, California 95616, USA

[†]Department of Physics and Astronomy, University of California, Davis, California 95616, USA

[‡]School of Electrical and Computer Engineering, Cornell University, Ithaca, New York 14850, USA

Contents

1	Introduction	2
2	Notation and background	8
2.1	Hilbert–Schmidt distance	8
2.2	Review of destructive SWAP test	9
3	Quantum algorithms for testing symmetries	12
3.1	Testing symmetries of states	12
3.2	Estimating the Hilbert–Schmidt distance of the Choi states of channels	14
3.3	Testing symmetries of channels	18
3.4	Testing symmetries of Lindbladians	20
4	Simulations	22
4.1	Amplitude damping channel	23
4.1.1	Dependence of X asymmetry measure on Γt	24
4.1.2	Amplitude damping channel simulation results	27
4.2	XX Spin chain	29
4.2.1	Spin-chain asymmetries as a function of Γt	30
4.2.2	Spin-chain simulation results	31
5	Measurements: Estimating Hilbert–Schmidt distance and testing symmetries	33
5.1	Estimating the Hilbert–Schmidt distance of the Choi states of measurement channels	34
5.2	Testing symmetries of measurement channels	37
6	Conclusion and discussion	38

1 Introduction

Symmetry is a fundamental concept in physics, simplifying our understanding of the physical world [22, 27]. In quantum mechanics especially, symmetry is helpful for determining which physical transitions are allowed [74, 1, 3] or in reducing the number of degrees of freedom needed to express a given physical system, thus making it easier to solve equations or optimization problems. In practical considerations, the interaction of the system with the environment can lead to a loss of symmetry, or yet, enforce certain

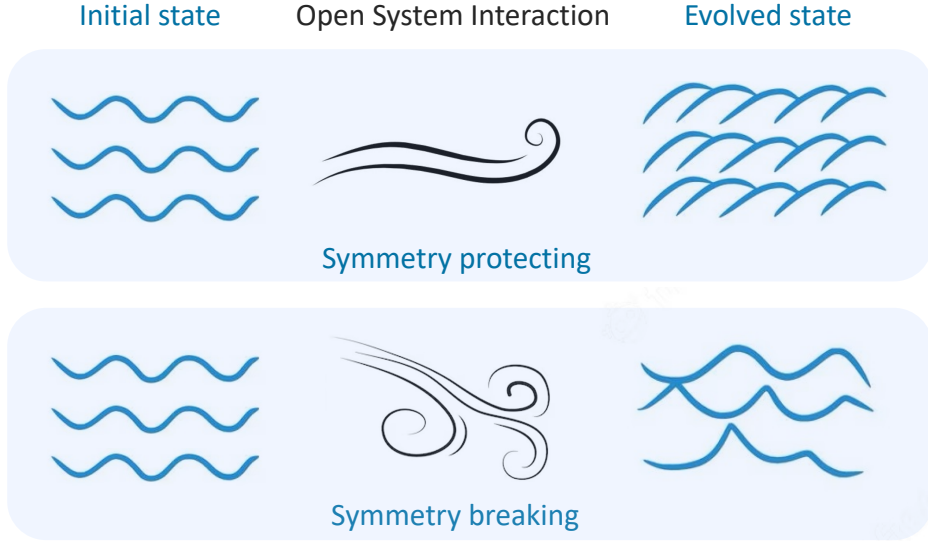


Figure 1: Interactions of systems with the environment can be symmetry preserving or symmetry breaking. The figure depicts an illustrative example of water waves interacting with wind that blows along different directions, potentially preserving or breaking the initial symmetry. In the first example (top), the wind preserves the symmetric structure of the water waves, so that the wind acts as a covariant channel, while in the second example (bottom), the wind is too chaotic, breaks the symmetry, and thus does not act as a covariant channel.

symmetries (Figure 1). As such, the concept of symmetry has carried over to quantum information processing [50], for understanding phenomena like entanglement [73, 19, 16, 17, 18, 12], coherence [48, 53, 62], and reference frames [3, 26]. The essential role of symmetry has elevated the concept itself to the status of a quantum resource theory [51, 52], in which objects possessing symmetry are considered freely available and those that break symmetry have value. Most recently, symmetry is being used in quantum machine learning to improve the trainability of learning algorithms [43, 54, 61].

Motivated by its fundamental role in physics and related fields, the authors of [40, 42] (cf. [39]) developed several quantum algorithms for testing symmetry of states, Hamiltonians, channels, and measurements on quantum computers, and a sequel paper places the related problems in the context of quantum computational complexity theory [41]. A number of these algorithms are efficiently realizable on quantum computers, while others have computational complexity provably beyond that of the standard BQP com-

plexity class and thus are believed to be difficult even for quantum computers to solve (here, BQP stands for bounded error quantum polynomial time; see [71, 69] for reviews on quantum computational complexity theory). Another contribution of [40] was to develop variational quantum algorithms for these more difficult problems, by replacing the operations of an unbounded “prover” with parameterized quantum circuits; this approach works well in certain instances but does not lead to provable computational runtimes (see [8, 4] for reviews of variational quantum algorithms).

One of the main contributions of the present paper is to develop alternative symmetry-testing algorithms that can be efficiently implemented on quantum computers. In contrast to the prior approaches from [40, 42], we modify the measure being estimated by a quantum computer. Whereas all of the algorithms from [40] estimate symmetry measures based on fidelity [68], here we develop algorithms that estimate asymmetry measures based on the Hilbert–Schmidt distance. Since estimating fidelity is considered to be a difficult problem for a quantum computer (more precisely, complete for a complexity class called quantum statistical zero knowledge [70]), while estimating the Hilbert–Schmidt distance is considered easy for a quantum computer (more precisely, complete for BQP [59]), it is expected that several of the symmetry testing algorithms from [40] are difficult for a quantum computer while the symmetry testing algorithms developed here are easy for a quantum computer to execute.

In our paper, we develop efficient symmetry testing algorithms for a number of scenarios involving open quantum systems. Specifically, our contributions consist of the following:

1. Given a state ρ and a unitary representation $\{U(g)\}_{g \in G}$ of a group G , our first algorithm estimates the following asymmetry measure:

$$\frac{1}{|G|} \sum_{g \in G} \|[U(g), \rho]\|_2^2, \quad (1)$$

where

$$\|A\|_2 := \sqrt{\text{Tr}[A^\dagger A]} \quad (2)$$

is the Hilbert–Schmidt norm of an operator A . This measure is a faithful asymmetry measure, in the sense that it is equal to zero if and only if $[U(g), \rho] = 0$ for all $g \in G$, the latter being the defining condition for symmetry of the state ρ with respect to the representation $\{U(g)\}_{g \in G}$ [3, 26, 50].

2. Given a quantum channel \mathcal{N} and a unitary channel representation $\{\mathcal{U}(g)\}_{g \in G}$ of a group G , where $\mathcal{U}(g)(\cdot) := U(g)(\cdot)U(g)^\dagger$, our next algorithm estimates the following asymmetry measure:

$$\frac{1}{|G|} \sum_{g \in G} \left\| (\text{id} \otimes [\mathcal{U}(g), \mathcal{N}])(\Phi^d) \right\|_2^2, \quad (3)$$

where id denotes the identity superoperator, $[\mathcal{U}(g), \mathcal{N}]$ represents the superoperator commutator (see, e.g., [3, Section II-C]), defined for superoperators \mathcal{A} and \mathcal{B} as

$$[\mathcal{A}, \mathcal{B}] := \mathcal{A} \circ \mathcal{B} - \mathcal{B} \circ \mathcal{A}, \quad (4)$$

and

$$\Phi^d := \frac{1}{d} \sum_{i,j} |i\rangle\langle j| \otimes |i\rangle\langle j| \quad (5)$$

is the standard maximally entangled state of Schmidt rank d . Thus,

$$\begin{aligned} (\text{id} \otimes [\mathcal{U}(g), \mathcal{N}])(\Phi^d) = \\ (\text{id} \otimes (\mathcal{U}(g) \circ \mathcal{N}))(\Phi^d) - (\text{id} \otimes (\mathcal{N} \circ \mathcal{U}(g)))(\Phi^d). \end{aligned} \quad (6)$$

As we show later on, the measure in (3) is a faithful asymmetry measure, in the sense that it is equal to zero if and only if

$$[\mathcal{U}(g), \mathcal{N}] = 0 \quad \forall g \in G, \quad (7)$$

or, equivalently, if and only if

$$\mathcal{U}(g) \circ \mathcal{N} = \mathcal{N} \circ \mathcal{U}(g) \quad \forall g \in G. \quad (8)$$

The latter is the defining condition for covariance symmetry of the channel \mathcal{N} with respect to the unitary channel representation $\{\mathcal{U}(g)\}_{g \in G}$ [33, 50]. In words, the equality above means that the channel \mathcal{N} commutes with every unitary channel representation $\mathcal{U}(g)$ of a group element $g \in G$. Our algorithm for this task builds on an efficient subroutine for estimating the Hilbert–Schmidt distance of the Choi states of two quantum channels, which may be of independent interest for other purposes in quantum computing.

3. As a special case of the above, we consider testing covariance symmetry of measurement channels, which have the form $\rho \rightarrow \mathcal{M}(\rho) :=$

$\sum_x \text{Tr}[M_x \rho] |x\rangle\langle x|$, where $\{M_x\}_x$ is a positive operator-valued measure and $\{|x\rangle\}_x$ is an orthonormal basis that encodes the measurement outcome. Specifically, we provide an algorithm that estimates the following asymmetry measure:

$$\frac{1}{|G|} \sum_{g \in G} \left\| \Phi^{\mathcal{M} \circ \mathcal{U}(g)} - \Phi^{\mathcal{W}(g) \circ \mathcal{M}} \right\|_2^2, \quad (9)$$

where $\{\mathcal{U}(g)\}_{g \in G}$ and $\{\mathcal{W}(g)\}_{g \in G}$ are unitary channel representations of a group G , with the latter realizing a shift of the measurement outcome as

$$\mathcal{W}(g)(|x\rangle\langle x|) = |\pi_g(x)\rangle\langle \pi_g(x)|, \quad (10)$$

for π_g a permutation. As discussed later on, this asymmetry measure is equal to zero if and only if the measurement is covariant [14, 34], i.e., such that $\mathcal{U}(g)(M_x)$ is an element of the POVM for all $g \in G$. Here again our algorithm builds on an efficient subroutine for estimating the Hilbert–Schmidt distance between two measurement channels, which we show is easier to perform than the aforementioned subroutine for general channels with quantum inputs and quantum outputs. We also believe that this subroutine should be of independent interest for other purposes in quantum computing.

As a particular application of our algorithm for estimating (3), we investigate the symmetry of Lindbladian evolutions, i.e., evolutions that correspond to the solution of the well known Lindblad master equation [47]:

$$\frac{\partial \rho}{\partial t} = \mathcal{L}(\rho) := -i[H, \rho] + \sum_k L_k \rho L_k^\dagger - \frac{1}{2} \{L_k^\dagger L_k, \rho\}, \quad (11)$$

where H is a Hamiltonian, $\{L_k\}_k$ is a set of Lindblad operators, and \mathcal{L} is a superoperator known as the Lindbladian. It is well known that the solution of (11) is the following quantum channel:

$$e^{\mathcal{L}t}(\rho) = \sum_{n=0}^{\infty} \frac{\mathcal{L}^n(\rho)t^n}{n!}, \quad (12)$$

where \mathcal{L}^n denotes n repeated applications of the superoperator \mathcal{L} . We accomplish symmetry testing of a Lindbladian \mathcal{L} by employing our algorithm for estimating (3) with the substitution $\mathcal{N} = e^{\mathcal{L}t}$, and later on, we remark on how symmetry testing of the channel $e^{\mathcal{L}t}$ is equivalent to symmetry testing of the Lindbladian \mathcal{L} .

Similar to how understanding symmetries of Hamiltonians can be helpful for deducing which physical transitions are allowed and which are not, the same can be said for understanding symmetries of the more general Lindbladian evolutions. As a particular example of this phenomenon, consider a Lindbladian in which the Hamiltonian is the photon number operator [25] and there is one Lindblad operator, which is also the photon number operator. Then the only states that are invariant under the resulting channel $e^{\mathcal{L}t}$ are the photon number states and mixtures thereof, because every other state becomes dephased by this evolution. Thus, under these dynamics and for long times, it is not possible to transition from a probabilistic mixture of photon number states to a coherent superposition of them, the latter of which is resourceful for estimation tasks in quantum metrology [67]. More generally, our algorithm is helpful for understanding symmetries of Lindbladian evolutions that are efficiently realizable on quantum computers, by means of any of the several quantum algorithms that have been proposed for simulating open systems dynamics [9, 13, 36, 60, 65] (see [55] for a review).

Before proceeding with the content of our paper, we note here that the symmetry testing quantum algorithms proposed here, like those from [40, 42], are most useful in the regime in which the states, channels, Lindbladians, or measurements being tested, as well as the group representation unitaries being considered, involve a large number of qubits and are non-trivial. In this regime, it is likely not possible to simulate these tests efficiently by means of a classical computer, as shown in [42, 41], based on the conjecture that the complexity class BQP strictly contains the complexity class BPP (the latter being the class of problems that are efficiently implementable on a classical probabilistic computer). The previous statement, less formally, is equivalent to the widespread belief that quantum computers, in principle, are generally more powerful than classical computers. Furthermore, it is certainly of interest to employ quantum computers for the task of learning symmetries (see, e.g., [49]), and we consider the ability to test symmetries to be an important component of the learning process (either while the learning is occurring or after learning has completed, as a way of testing whether the learned symmetry is indeed correct).

In the rest of our paper, we provide details of our algorithms and evaluate their performance for some exemplary physical systems of interest. In particular, Section 2 reviews some basic notation and concepts used throughout the rest of our paper. Section 3 develops the theory behind our quantum algorithms for testing symmetry of states (Section 3.1), channels (Section 3.3), and Lindbladians (Section 3.4). As part of our algorithm for testing symmetries of channels, we develop an efficient subroutine for estimating the

Hilbert–Schmidt distance of the Choi states of two quantum channels (Section 3.2), which may be of independent interest for other purposes in quantum computing. Specifically, this algorithm significantly reduces the number of qubits needed for the estimation, when compared to a naive approach to this problem. In Section 4, we test out our algorithms for estimating symmetries of Lindbladians for two example scenarios, using Qiskit’s noiseless and noisy simulators [66]. Section 5 particularizes the development for quantum channels to the case of quantum measurement channels, proposing both a procedure for estimating the Hilbert–Schmidt distance of the Choi states of two such channels, as well as for estimating an asymmetry measure for a given measurement channel. Finally, in Section 6, we conclude with a summary of our contributions, along with a discussion of prospects for implementing the developed algorithms on near-term quantum hardware.

2 Notation and background

This section provides some notation and background used throughout the rest of our paper. See [28, 75, 72, 35, 37] for further background on quantum information. A quantum state (density operator) is described by a positive semi-definite operator with unit trace. A quantum channel is a completely positive, trace-preserving superoperator. The Choi state $\Phi^{\mathcal{N}}$ of a channel \mathcal{N} is given by sending one share of a maximally entangled state Φ^d , defined in (5), through the channel:

$$\Phi^{\mathcal{N}} := (\text{id} \otimes \mathcal{N})(\Phi^d), \quad (13)$$

where we have assumed that the input space of \mathcal{N} is d -dimensional.

2.1 Hilbert–Schmidt distance

The Hilbert–Schmidt distance between two states ρ and σ , induced by the norm in (2), is given by $\|\rho - \sigma\|_2$. It is faithful, in the sense that $\|\rho - \sigma\|_2 = 0$ if and only if $\rho = \sigma$. It obeys the data-processing inequality for unital channels [58], but it does not obey it in general [57]; that is, the following inequality holds whenever \mathcal{N} is a unital channel (satisfying $\mathcal{N}(I) = I$, where I is the identity operator):

$$\|\rho - \sigma\|_2 \geq \|\mathcal{N}(\rho) - \mathcal{N}(\sigma)\|_2. \quad (14)$$

When ρ and σ are multi-qubit states and one can prepare many copies of them on a quantum computer, it is easy to estimate the square of their

Hilbert–Schmidt distance by means of the destructive SWAP test (reviewed in Section 2.2 below). This follows by considering the expansion

$$\|\rho - \sigma\|_2^2 = \text{Tr}[\rho^2] + \text{Tr}[\sigma^2] - 2 \text{Tr}[\rho\sigma], \quad (15)$$

and the algorithm reviewed in the next section. In fact, it is known that estimating the Hilbert–Schmidt distance of quantum states ρ and σ prepared by circuits is a BQP-complete problem [59, Theorem 14], so that this problem captures and is equivalent to the full power of quantum computation.

2.2 Review of destructive SWAP test

Let us define the unitary swap operator as

$$\text{SWAP} := \sum_{i,j} |i\rangle\langle j| \otimes |j\rangle\langle i|, \quad (16)$$

and note the following identity:

$$\text{Tr}[CD] = \text{Tr}[\text{SWAP}(C \otimes D)], \quad (17)$$

which holds for arbitrary linear operators C and D and plays a key role in our algorithms that follow. Recall that, if the SWAP operator acts on qubit systems, then

$$\text{SWAP} = \sum_{i,j \in \{0,1\}} (-1)^{ij} \Phi^{ij}, \quad (18)$$

where

$$\Phi^{00} = \Phi^+, \quad \Phi^{10} = \Phi^-, \quad \Phi^{01} = \Psi^+, \quad \Phi^{11} = \Psi^-. \quad (19)$$

In the above, $\Phi^+ \equiv |\Phi^+\rangle\langle\Phi^+|$, $\Phi^- \equiv |\Phi^-\rangle\langle\Phi^-|$, $\Psi^+ \equiv |\Psi^+\rangle\langle\Psi^+|$, and $\Psi^- \equiv |\Psi^-\rangle\langle\Psi^-|$ are the standard Bell states, defined through

$$|\Phi^\pm\rangle := \frac{1}{\sqrt{2}} (|00\rangle \pm |11\rangle), \quad |\Psi^\pm\rangle := \frac{1}{\sqrt{2}} (|01\rangle \pm |10\rangle). \quad (20)$$

This means that the SWAP observable for qubits can be measured by means of a Bell measurement and classical post-processing, a fact that is used in the destructive SWAP test method for measuring the SWAP observable [24] (see also [6, 64] and Eqs. (26)–(37) of [59] for a review of this method).

For convenience, we briefly review the destructive SWAP test [24] for estimating the overlap term $\text{Tr}[\rho\sigma]$, where ρ and σ are n -qubit states, with ρ

a state of qubits $1, \dots, n$ and σ a state of qubits $n+1, \dots, 2n$. The idea behind it is a consequence of the following observation:

$$\mathrm{Tr}[\rho\sigma] = \mathrm{Tr}[\mathrm{SWAP}^{(n)}(\rho \otimes \sigma)] \quad (21)$$

$$= \sum_{\vec{k}, \vec{\ell} \in \{0,1\}^n} (-1)^{\vec{k} \cdot \vec{\ell}} \mathrm{Tr}[\Phi^{\vec{k}\vec{\ell}}(\rho \otimes \sigma)], \quad (22)$$

where

$$\vec{k} \equiv (k_1, k_2, \dots, k_n), \quad \vec{\ell} \equiv (\ell_1, \ell_2, \dots, \ell_n), \quad (23)$$

$$\Phi^{\vec{k}\vec{\ell}} \equiv \Phi_{1,n+1}^{k_1\ell_1} \otimes \Phi_{2,n+2}^{k_2\ell_2} \otimes \dots \otimes \Phi_{n,2n}^{k_n\ell_n}, \quad (24)$$

and we used the identity in (18), as well as the fact that

$$\mathrm{SWAP}^{(n)} = \mathrm{SWAP}^{\otimes n} \quad (25)$$

$$= \left(\sum_{k_1, \ell_1} (-1)^{k_1\ell_1} \Phi_{1,n+1}^{k_1\ell_1} \right) \otimes \dots \otimes \left(\sum_{k_n, \ell_n} (-1)^{k_n\ell_n} \Phi_{n,2n}^{k_n\ell_n} \right) \quad (26)$$

$$= \sum_{\vec{k}, \vec{\ell} \in \{0,1\}^n} (-1)^{\vec{k} \cdot \vec{\ell}} \Phi^{\vec{k}\vec{\ell}}. \quad (27)$$

By setting $Z \equiv (\vec{K}, \vec{L})$ to be a multi-indexed random variable taking the value $(-1)^{\vec{k} \cdot \vec{\ell}}$ with probability

$$p(\vec{k}, \vec{\ell}) := \mathrm{Tr}[\Phi^{\vec{k}\vec{\ell}}(\rho \otimes \sigma)], \quad (28)$$

we find from (21)–(22) that its expectation is given by

$$\mathbb{E}[Z] = \sum_{\vec{k}, \vec{\ell} \in \{0,1\}^n} (-1)^{\vec{k} \cdot \vec{\ell}} \mathrm{Tr}[\Phi^{\vec{k}\vec{\ell}}(\rho \otimes \sigma)] = \mathrm{Tr}[\rho\sigma]. \quad (29)$$

This observation then leads to the following quantum algorithm (destructive SWAP test) for estimating $\mathrm{Tr}[\rho\sigma]$, within additive error ε and with success probability at least $1 - \delta$, where $\varepsilon > 0$ and $\delta \in (0, 1)$.

Algorithm 1 *Given are quantum circuits to prepare the n -qubit states ρ and σ .*

1. Fix $\varepsilon > 0$ and $\delta \in (0, 1)$. Set $T \geq \frac{2}{\varepsilon^2} \ln(\frac{2}{\delta})$ and set $t = 1$.

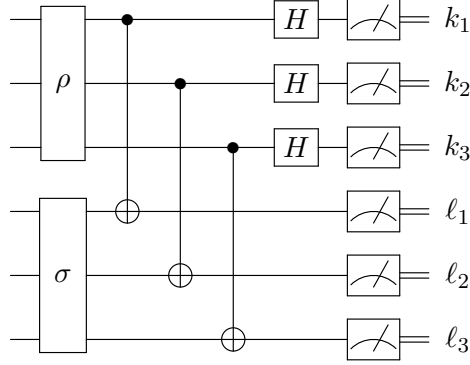


Figure 2: Depiction of the core quantum subroutine given in Steps 2.-3. of Algorithm 1, for the three-qubit states ρ and σ . This algorithm estimates the overlap $\text{Tr}[\rho\sigma]$.

2. Prepare the states ρ and σ on $2n$ qubits (using the ordering specified in (24)).
3. Perform the Bell measurement $\{\Phi^{\vec{k}\vec{\ell}}\}_{\vec{k}\vec{\ell}}$ on the $2n$ qubits, which leads to the measurement outcomes \vec{k} and $\vec{\ell}$.
4. Set $Z_t = (-1)^{\vec{k}\cdot\vec{\ell}}$.
5. Increment t .
6. Repeat Steps 2.-5. until $t > T$ and then output $\bar{Z} := \frac{1}{T} \sum_{t=1}^T Z_t$ as an estimate of $\text{Tr}[\rho\sigma]$.

Figure 2 depicts the core quantum subroutine of Algorithm 1. By the Hoeffding inequality (recalled as Theorem 1 below), we are guaranteed that the output of Algorithm 1 satisfies

$$\Pr[|\bar{Z} - \text{Tr}[\rho\sigma]| \leq \varepsilon] \geq 1 - \delta, \quad (30)$$

due to the choice $T \geq \frac{2}{\varepsilon^2} \ln(\frac{2}{\delta})$.

Clearly, by the expansion in (15) and repeating Algorithm 1 three times, one can use $O(\frac{1}{\varepsilon^2} \ln(\frac{1}{\delta}))$ samples of ρ and σ in order to obtain an estimate of (15) within additive error $\varepsilon > 0$ and with success probability not smaller than $1 - \delta$, where $\delta \in (0, 1)$.

Theorem 1 (Hoeffding Inequality [29]) *Suppose that we are given T independent samples Y_1, \dots, Y_T of a bounded random variable Y taking values*

in the interval $[a, b]$ and having mean μ . Set $\overline{Y_T} := \frac{1}{T}(Y_1 + \dots + Y_T)$ to be the sample mean. Let $\varepsilon > 0$ be the desired accuracy, and let $1 - \delta$ be the desired success probability, where $\delta \in (0, 1)$. Then

$$\Pr[|\overline{Y_T} - \mu| \leq \varepsilon] \geq 1 - \delta, \quad (31)$$

as long as $T \geq \frac{M^2}{2\varepsilon^2} \ln(\frac{2}{\delta})$, where $M := b - a$.

3 Quantum algorithms for testing symmetries

3.1 Testing symmetries of states

Let us now introduce a simple quantum algorithm for testing symmetry of the state ρ with respect to the unitary representation $\{U(g)\}_{g \in G}$ of a group G . Specifically, the goal is to estimate the normalized commutator norm in (1). As discussed around (1), this asymmetry measure is equal to zero if and only if $[U(g), \rho] = 0$ for all $g \in G$. To start off, we establish the following lemma, which provides a direct link between the asymmetry measure in (1), and an approach we can use for estimating it on a quantum computer.

Lemma 1 *Given a state ρ and a unitary representation $\{U(g)\}_{g \in G}$ of a group G , the following equality holds:*

$$\frac{1}{|G|} \sum_{g \in G} \|[U(g), \rho]\|_2^2 = 2 (\text{Tr}[\rho^2] - \text{Tr}[\rho \mathcal{T}_G(\rho)]), \quad (32)$$

where \mathcal{T}_G is the twirl channel given by

$$\mathcal{T}_G(\cdot) := \frac{1}{|G|} \sum_{g \in G} U(g)(\cdot)U(g)^\dagger. \quad (33)$$

Proof. Consider the following equalities:

$$\|[U(g), \rho]\|_2^2 = \|\rho U(g) - U(g)\rho\|_2^2 \quad (34)$$

$$= \left\| \rho - U(g)\rho U(g)^\dagger \right\|_2^2 \quad (35)$$

$$= \text{Tr}[\rho^2] + \text{Tr}[(U(g)\rho U(g)^\dagger)^2] - 2 \text{Tr}[\rho U(g)\rho U(g)^\dagger] \quad (36)$$

$$= 2 \left(\text{Tr}[\rho^2] - \text{Tr}[\rho U(g)\rho U(g)^\dagger] \right), \quad (37)$$

where the second equality is due to the unitary invariance of the Hilbert–Schmidt norm, the third from the expansion in (15), and the final one from cyclicity of trace. Thus, we see that

$$\frac{1}{|G|} \sum_{g \in G} \|[U(g), \rho]\|_2^2 = \frac{1}{|G|} \sum_{g \in G} 2 \left(\text{Tr}[\rho^2] - \text{Tr}[\rho U(g) \rho U(g)^\dagger] \right) \quad (38)$$

$$= 2 \left(\text{Tr}[\rho^2] - \text{Tr}[\rho \mathcal{T}_G(\rho)] \right), \quad (39)$$

concluding the proof. ■

Now suppose that the state ρ is an n -qubit state and efficiently preparable on a quantum computer, either by a quantum circuit or other means, and that, for all $g \in G$, there exists a circuit that efficiently realizes the n -qubit unitary $U(g)$. Then the idea for estimating the asymmetry measure in (1) is simple: Perform the destructive SWAP test (Algorithm 1) to estimate $\text{Tr}[\rho^2]$ and perform the same test, using instead ρ and its twirled version $\mathcal{T}_G(\rho)$, to estimate $\text{Tr}[\rho \mathcal{T}_G(\rho)]$. When estimating the latter term, we modify Algorithm 1 to be as follows:

Algorithm 2 *Given is a quantum circuit to prepare the n -qubit state ρ and circuits to generate the unitaries in the representation $\{U(g)\}_{g \in G}$.*

1. Fix $\varepsilon > 0$ and $\delta \in (0, 1)$. Set $T \geq \frac{2}{\varepsilon^2} \ln\left(\frac{2}{\delta}\right)$ and set $t = 1$.
2. Pick $g \in G$ uniformly at random. Prepare the states ρ and $U(g)\rho U(g)^\dagger$ on $2n$ qubits (using the ordering specified in (24)).
3. Perform the Bell measurement $\{\Phi_{\vec{k}\vec{\ell}}^{\vec{k}\vec{\ell}}\}_{\vec{k}\vec{\ell}}$ on the $2n$ qubits, which leads to the measurement outcomes \vec{k} and $\vec{\ell}$.
4. Set $Z_t = (-1)^{\vec{k}\cdot\vec{\ell}}$.
5. Increment t .
6. Repeat Steps 2.-5. until $t > T$ and then output $\bar{Z} := \frac{1}{T} \sum_{t=1}^T Z_t$ as an estimate of $\text{Tr}[\rho \mathcal{T}_G(\rho)]$.

Thus, by combining the estimates of $\text{Tr}[\rho^2]$ and $\text{Tr}[\rho \mathcal{T}_G(\rho)]$ according to (32), it follows that this approach uses $O\left(\frac{1}{\varepsilon^2} \ln\left(\frac{1}{\delta}\right)\right)$ samples of ρ in order to obtain an estimate of the asymmetry measure in (1) within additive error $\varepsilon > 0$ and with success probability not smaller than $1 - \delta$, where $\delta \in (0, 1)$.

3.2 Estimating the Hilbert–Schmidt distance of the Choi states of channels

Let us now introduce a method for estimating the Hilbert–Schmidt distance between the Choi states of two quantum channels, as a generalization of the destructive SWAP test used for estimating the Hilbert–Schmidt distance between two states. This algorithm has applications beyond symmetry testing, for example, in quantum channel compilation as a generalization of compiling states (see [21] for the latter).

To begin with, recall that two channels \mathcal{N} and \mathcal{M} are equal if and only if their Choi states are equal [75, Section 4.4.2]; i.e.,

$$\mathcal{N} = \mathcal{M} \quad \Leftrightarrow \quad \Phi^{\mathcal{N}} = \Phi^{\mathcal{M}}, \quad (40)$$

where the Choi states $\Phi^{\mathcal{N}}$ and $\Phi^{\mathcal{M}}$ are defined in (13). One way to determine whether the equality above holds approximately is to employ the Hilbert–Schmidt distance of the Choi states:

$$\|\Phi^{\mathcal{N}} - \Phi^{\mathcal{M}}\|_2, \quad (41)$$

where the Hilbert–Schmidt norm is defined in (2). This is due to the positive definiteness or faithfulness of the norm, i.e.,

$$\|\Phi^{\mathcal{N}} - \Phi^{\mathcal{M}}\|_2 = 0 \quad \Leftrightarrow \quad \Phi^{\mathcal{N}} = \Phi^{\mathcal{M}}. \quad (42)$$

Using the expansion in (15), consider that

$$\|\Phi^{\mathcal{N}} - \Phi^{\mathcal{M}}\|_2^2 = \text{Tr}[(\Phi^{\mathcal{N}})^2] + \text{Tr}[(\Phi^{\mathcal{M}})^2] - 2 \text{Tr}[\Phi^{\mathcal{N}}\Phi^{\mathcal{M}}]. \quad (43)$$

The following lemma gives a way of rewriting the overlap $\text{Tr}[\Phi^{\mathcal{N}}\Phi^{\mathcal{M}}]$ in terms of the SWAP observable, and it is critical to our simplified approach for estimating the Hilbert–Schmidt distance between the Choi states of two channels.

Lemma 2 *Let \mathcal{N} and \mathcal{M} be channels with Choi states $\Phi^{\mathcal{N}}$ and $\Phi^{\mathcal{M}}$, respectively, and d -dimensional inputs. Then*

$$\text{Tr}[\Phi^{\mathcal{N}}\Phi^{\mathcal{M}}] = \frac{1}{d^2} \text{Tr}[\text{SWAP}(\mathcal{N} \otimes \mathcal{M})(\text{SWAP})]. \quad (44)$$

Proof. Consider that

$$\text{Tr}[\Phi^{\mathcal{N}}\Phi^{\mathcal{M}}] = \text{Tr}[(\text{id} \otimes \mathcal{N})(\Phi^d)(\text{id} \otimes \mathcal{M})(\Phi^d)] \quad (45)$$

$$= \frac{1}{d^2} \sum_{i,j,k,\ell} \text{Tr}[(|i\rangle\langle j| \otimes \mathcal{N}(|i\rangle\langle j|)) (|k\rangle\langle \ell| \otimes \mathcal{M}(|k\rangle\langle \ell|))] \quad (46)$$

$$= \frac{1}{d^2} \sum_{i,j,k,\ell} \langle \ell|i\rangle\langle j|k\rangle \otimes \text{Tr}[\mathcal{N}(|i\rangle\langle j|)\mathcal{M}(|k\rangle\langle \ell|)] \quad (47)$$

$$= \frac{1}{d^2} \sum_{i,j} \text{Tr}[\mathcal{N}(|i\rangle\langle j|)\mathcal{M}(|j\rangle\langle i|)] \quad (48)$$

$$= \frac{1}{d^2} \sum_{i,j} \text{Tr}[\text{SWAP}(\mathcal{N} \otimes \mathcal{M})(|i\rangle\langle j| \otimes |j\rangle\langle i|)] \quad (49)$$

$$= \frac{1}{d^2} \text{Tr}[\text{SWAP}(\mathcal{N} \otimes \mathcal{M})(\text{SWAP})]. \quad (50)$$

The penultimate equality follows from (17). ■

Now suppose that the channels \mathcal{N} and \mathcal{M} each accept n qubits as input and output m qubits. Then each of the terms in (43) can be efficiently measured on a quantum computer. For example, to measure the last term $\text{Tr}[\Phi^{\mathcal{N}}\Phi^{\mathcal{M}}]$, one could prepare the tensor-product state $\Phi^{\mathcal{N}} \otimes \Phi^{\mathcal{M}}$ and then perform a destructive SWAP test, as recalled in Algorithm 1. This approach, which we consider to be a naive approach in light of Algorithm 3 below, requires $2(n+m)$ qubits in total, for a circuit width of $2(n+m)$ qubits. However, what follows as a consequence of Lemma 2 is that there is a simpler procedure for estimating $\text{Tr}[\Phi^{\mathcal{N}}\Phi^{\mathcal{M}}]$, which requires preparing only $2n$ qubits at the input and acting on $2m$ qubits at the output, and thus for a circuit width of $\max\{2n, 2m\}$ qubits.

Indeed, Lemma 2 establishes that

$$\text{Tr}[\Phi^{\mathcal{N}}\Phi^{\mathcal{M}}] = \frac{1}{2^{2n}} \text{Tr}[\text{SWAP}^{(m)}(\mathcal{N} \otimes \mathcal{M})(\text{SWAP}^{(n)})], \quad (51)$$

where the superscript notation explicitly indicates the number of qubits on which the swap operator acts. Next recall (25)–(27), which implies that

$$\begin{aligned} & \frac{1}{2^{2n}} \text{Tr}[\text{SWAP}^{(m)}(\mathcal{N} \otimes \mathcal{M})(\text{SWAP}^{(n)})] \\ &= \frac{1}{2^{2n}} \sum_{\vec{i}, \vec{j} \in \{0,1\}^m} \sum_{\vec{k}, \vec{\ell} \in \{0,1\}^n} (-1)^{\vec{i} \cdot \vec{j} + \vec{k} \cdot \vec{\ell}} \text{Tr}[\Phi^{\vec{i}\vec{j}}(\mathcal{N} \otimes \mathcal{M})(\Phi^{\vec{k}\vec{\ell}})], \end{aligned} \quad (52)$$

where

$$\vec{i} \equiv (i_1, i_2, \dots, i_m), \quad \vec{j} \equiv (j_1, j_2, \dots, j_m), \quad (53)$$

$$\vec{k} \equiv (k_1, k_2, \dots, k_n), \quad \vec{\ell} \equiv (\ell_1, \ell_2, \dots, \ell_n), \quad (54)$$

$$\Phi^{\vec{i}\vec{j}} \equiv \Phi_{1,m+1}^{i_1 j_1} \otimes \Phi_{2,m+2}^{i_2 j_2} \otimes \dots \otimes \Phi_{m,2m}^{i_m j_m}, \quad (55)$$

$$\Phi^{\vec{k}\vec{\ell}} \equiv \Phi_{1,n+1}^{k_1 \ell_1} \otimes \Phi_{2,n+2}^{k_2 \ell_2} \otimes \dots \otimes \Phi_{n,2n}^{k_n \ell_n}. \quad (56)$$

Eq. (52) and Lemma 2 are the key insights that lead to a simplified quantum algorithm for estimating the term $\text{Tr}[\Phi^{\mathcal{N}}\Phi^{\mathcal{M}}]$, which requires only $2n$ qubits at the input and $2m$ qubits at the output. In the above, we have implicitly used the following ordering: the channel \mathcal{N} acts on input qubits $1, \dots, n$ and produces output qubits $1, \dots, m$, the channel \mathcal{M} acts on input qubits $n+1, \dots, 2n$ and produces output qubits $m+1, \dots, 2m$, and the qubits for the Bell states are labeled as subscripts above. By setting $Y \equiv (\vec{I}, \vec{J}, \vec{K}, \vec{L})$ to be a multi-indexed random variable taking the value $(-1)^{\vec{i}\cdot\vec{j}+\vec{k}\cdot\vec{\ell}}$ with probability

$$p(\vec{k}, \vec{\ell}, \vec{i}, \vec{j}) = p(\vec{i}, \vec{j} | \vec{k}, \vec{\ell}) p(\vec{k}, \vec{\ell}), \quad (57)$$

where

$$p(\vec{k}, \vec{\ell}) := \frac{1}{2^{2n}}, \quad (58)$$

$$p(\vec{i}, \vec{j} | \vec{k}, \vec{\ell}) := \text{Tr}[\Phi^{\vec{i}\vec{j}} (\mathcal{N} \otimes \mathcal{M}) (\Phi^{\vec{k}\vec{\ell}})], \quad (59)$$

we find from (51)–(52) that its expectation is given by

$$\mathbb{E}[Y] = \frac{1}{2^{2n}} \text{Tr}[\text{SWAP}^{(m)} (\mathcal{N} \otimes \mathcal{M}) (\text{SWAP}^{(n)})] = \text{Tr}[\Phi^{\mathcal{N}}\Phi^{\mathcal{M}}]. \quad (60)$$

The observation in (60) then leads to the following quantum algorithm for estimating $\text{Tr}[\Phi^{\mathcal{N}}\Phi^{\mathcal{M}}]$, within additive error ε and with success probability not smaller than $1 - \delta$, where $\varepsilon > 0$ and $\delta \in (0, 1)$.

Algorithm 3 *Given are quantum circuits to implement the channels \mathcal{N} and \mathcal{M} .*

1. Fix $\varepsilon > 0$ and $\delta \in (0, 1)$. Set $T \geq \frac{2}{\varepsilon^2} \ln(\frac{2}{\delta})$ and set $t = 1$.
2. Generate the bit vectors \vec{k} and $\vec{\ell}$ uniformly at random.
3. Prepare the Bell state $\Phi^{\vec{k}\vec{\ell}}$ on $2n$ qubits (using the ordering specified in (56)).
4. Apply the tensor-product channel $\mathcal{N} \otimes \mathcal{M}$ (using the ordering specified after (56)).

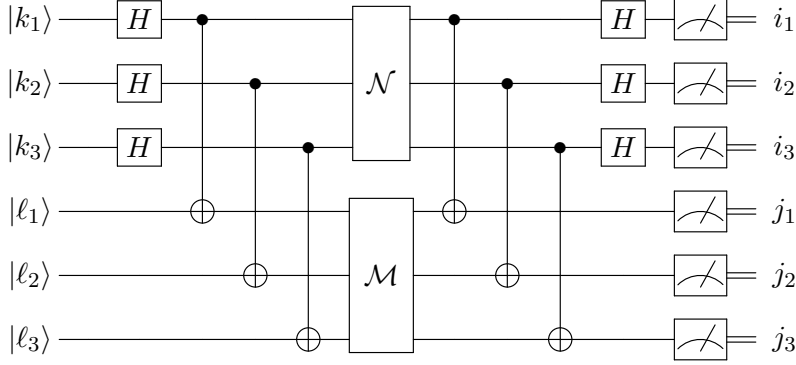


Figure 3: Depiction of the core quantum subroutine given in Steps 2.-5. of Algorithm 3, such that the quantum channels \mathcal{N} and \mathcal{M} have three-qubit inputs and outputs. This algorithm estimates the overlap $\text{Tr}[\Phi^{\mathcal{N}}\Phi^{\mathcal{M}}]$ of the Choi states of the channels. In this example, the algorithm begins by preparing the classical state $|k_1, k_2, k_3, \ell_1, \ell_2, \ell_3\rangle$, where the values $k_1, k_2, k_3, \ell_1, \ell_2, \ell_3$ are chosen uniformly at random, followed by a sequence of controlled NOTs and Hadamards. Before the channels are applied, the state is thus $|\Phi^{\vec{k}\vec{\ell}}\rangle$, as described in Algorithm 3. After the channels are applied, Bell measurements are performed, which lead to the classical bit string $i_1 i_2 i_3 j_1 j_2 j_3$. In the diagram, we depict the realization of the channels \mathcal{N} and \mathcal{M} as black boxes, but in a simulation of them, one might make use of additional environment qubits that are prepared and then discarded.

5. Perform the Bell measurement $\{\Phi^{\vec{i}\vec{j}}\}_{\vec{i}, \vec{j}}$ on the $2m$ output qubits, which leads to the measurement outcomes \vec{i} and \vec{j} .
6. Set $Y_t = (-1)^{\vec{i}\cdot\vec{j} + \vec{k}\cdot\vec{\ell}}$.
7. Increment t .
8. Repeat Steps 2.-7. until $t > T$ and then output $\bar{Y} := \frac{1}{T} \sum_{t=1}^T Y_t$ as an estimate of $\text{Tr}[\Phi^{\mathcal{N}}\Phi^{\mathcal{M}}]$.

Figure 3 depicts the core quantum subroutine of Algorithm 3. By the Hoeffding inequality (recalled as Theorem 1), we are guaranteed that the output of Algorithm 3 satisfies

$$\Pr[|\bar{Y} - \text{Tr}[\Phi^{\mathcal{N}}\Phi^{\mathcal{M}}]| \leq \varepsilon] \geq 1 - \delta, \quad (61)$$

due to the choice $T \geq \frac{2}{\varepsilon^2} \ln(\frac{2}{\delta})$.

By employing Algorithm 3 three times, we can thus estimate (43) within additive error ε and with success probability not smaller than $1 - \delta$, by using $O(\frac{1}{\varepsilon^2} \ln(\frac{1}{\delta}))$ samples of the channels \mathcal{N} and \mathcal{M} .

3.3 Testing symmetries of channels

In this section, we leverage the methods for estimating the Hilbert–Schmidt asymmetry measure for states (Section 3.1), as well as the method for estimating the Hilbert–Schmidt distance between the Choi states of channels (Section 3.2), in order to develop an approach for estimating the covariance symmetry of a quantum channel \mathcal{N} with respect to a unitary channel representation $\{\mathcal{U}(g)\}_{g \in G}$.

Recalling the superoperator commutator notation defined in (4), we are interested in estimating the following asymmetry measure:

$$\frac{1}{|G|} \sum_{g \in G} \left\| (\text{id} \otimes [\mathcal{U}(g), \mathcal{N}]) (\Phi^d) \right\|_2^2. \quad (62)$$

As discussed around (3), this asymmetry measure is equal to zero if and only if $\mathcal{N} \circ \mathcal{U}(g) = \mathcal{U}(g) \circ \mathcal{N}$ holds for every $g \in G$.

We begin with the following lemma:

Lemma 3 *Given a quantum channel \mathcal{N} and a unitary channel representation $\{\mathcal{U}(g)\}_{g \in G}$, the following equality holds:*

$$\begin{aligned} \frac{1}{|G|} \sum_{g \in G} \left\| (\text{id} \otimes [\mathcal{U}(g), \mathcal{N}]) (\Phi^d) \right\|_2^2 &= \frac{2}{d^2} \text{Tr}[\text{SWAP}(\mathcal{N} \otimes \mathcal{N})(\text{SWAP})] \\ &\quad - \frac{2}{d^2} \text{Tr} \left[\text{SWAP} \left(\frac{1}{|G|} \sum_{g \in G} (\mathcal{U}(g) \circ \mathcal{N}) \otimes (\mathcal{N} \circ \mathcal{U}(g)) \right) (\text{SWAP}) \right]. \end{aligned} \quad (63)$$

Proof. Consider that, for all $g \in G$,

$$\begin{aligned} &\left\| (\text{id} \otimes [\mathcal{U}(g), \mathcal{N}]) (\Phi^d) \right\|_2^2 \\ &= \left\| \Phi^{\mathcal{U}(g) \circ \mathcal{N}} - \Phi^{\mathcal{N} \circ \mathcal{U}(g)} \right\|_2^2 \end{aligned} \quad (64)$$

$$= \text{Tr}[(\Phi^{\mathcal{U}(g) \circ \mathcal{N}})^2] + \text{Tr}[(\Phi^{\mathcal{N} \circ \mathcal{U}(g)})^2] - 2 \text{Tr}[\Phi^{\mathcal{U}(g) \circ \mathcal{N}} \Phi^{\mathcal{N} \circ \mathcal{U}(g)}] \quad (65)$$

$$= 2 \left(\text{Tr}[(\Phi^{\mathcal{N}})^2] - \text{Tr}[\Phi^{\mathcal{U}(g) \circ \mathcal{N}} \Phi^{\mathcal{N} \circ \mathcal{U}(g)}] \right), \quad (66)$$

where we made use of the expansion in (15), as well as the equalities

$$\text{Tr}[(\Phi^{\mathcal{U}(g) \circ \mathcal{N}})^2] = \text{Tr}[(\Phi^{\mathcal{N}})^2], \quad \text{Tr}[(\Phi^{\mathcal{N} \circ \mathcal{U}(g)})^2] = \text{Tr}[(\Phi^{\mathcal{N}})^2]. \quad (67)$$

The equalities in (67) follow because

$$\text{Tr}[(\Phi^{\mathcal{U}(g) \circ \mathcal{N}})^2] = \text{Tr}[\{(\text{id} \otimes (\mathcal{U}(g) \circ \mathcal{N}))(\Phi^d)\}^2] \quad (68)$$

$$= \text{Tr}[\{(\text{id} \otimes \mathcal{N})(\Phi^d)\}^2] \quad (69)$$

$$= \text{Tr}[(\Phi^{\mathcal{N}})^2], \quad (70)$$

$$\text{Tr}[(\Phi^{\mathcal{N} \circ \mathcal{U}(g)})^2] = \text{Tr}[\{(\text{id} \otimes (\mathcal{N} \circ \mathcal{U}(g)))(\Phi^d)\}^2] \quad (71)$$

$$= \text{Tr}[\{(\mathcal{U}^T(g) \otimes \mathcal{N})(\Phi^d)\}^2] \quad (72)$$

$$= \text{Tr}[\{(\text{id} \otimes \mathcal{N})(\Phi^d)\}^2] \quad (73)$$

$$= \text{Tr}[(\Phi^{\mathcal{N}})^2]. \quad (74)$$

The equalities in (69) and (73) in turn follow because the function $\text{Tr}[\sigma^2]$ depends only on the eigenvalues of σ , and its eigenvalues are invariant under the action of a unitary channel. The equality in (72) follows from the transpose trick [75, Exercise 3.7.12]; i.e., the identity $(\text{id} \otimes \mathcal{U})(\Phi^d) = (\mathcal{U}^T \otimes \text{id})(\Phi^d)$ holds for every unitary channel \mathcal{U} , where the transpose channel is defined as $\mathcal{U}^T(\cdot) = U^T(\cdot)\bar{U}$, with \bar{U} the matrix realized from U by entrywise complex conjugation. Now employing Lemma 2, we can write

$$\text{Tr}[(\Phi^{\mathcal{N}})^2] = \frac{1}{d^2} \text{Tr}[\text{SWAP}(\mathcal{N} \otimes \mathcal{N})(\text{SWAP})], \quad (75)$$

$$\text{Tr}[\Phi^{\mathcal{U}(g) \circ \mathcal{N}} \Phi^{\mathcal{N} \circ \mathcal{U}(g)}] = \frac{1}{d^2} \text{Tr}[\text{SWAP}((\mathcal{U}(g) \circ \mathcal{N}) \otimes (\mathcal{N} \circ \mathcal{U}(g)))(\text{SWAP})], \quad (76)$$

which finally implies the claim in (63). ■

In order to estimate the channel asymmetry measure in (62), it follows from Lemma 3 that we can make use of Algorithm 3 to estimate the following two quantities:

$$\frac{1}{d^2} \text{Tr}[\text{SWAP}(\mathcal{N} \otimes \mathcal{N})(\text{SWAP})], \quad (77)$$

$$\frac{1}{d^2} \text{Tr} \left[\text{SWAP} \left(\frac{1}{|G|} \sum_{g \in G} (\mathcal{U}(g) \circ \mathcal{N}) \otimes (\mathcal{N} \circ \mathcal{U}(g)) \right) (\text{SWAP}) \right], \quad (78)$$

subtract the estimates, and multiply by two. For estimating the quantity in (78), similar to how we did in Algorithm 2, we can slightly revise Algorithm 3 such that $g \in G$ is chosen uniformly at random in each step.

Remark 1 *More generally, a quantum channel \mathcal{N} can possess a covariance symmetry of the following form:*

$$\mathcal{N} \circ \mathcal{U}(g) = \mathcal{V}(g) \circ \mathcal{N} \quad \forall g \in G, \quad (79)$$

where $\{\mathcal{U}(g)\}_{g \in G}$ and $\{\mathcal{V}(g)\}_{g \in G}$ are unitary channel representations of a group G . This more general symmetry occurs especially in the case in which the dimensions of the channel input and output differ (as is the case, e.g., for the quantum erasure channel [75]).

We note here that all of the observations from this section apply to this more general case. Namely, the asymmetry measure from (62) generalizes to

$$\begin{aligned} \frac{1}{|G|} \sum_{g \in G} \left\| \Phi^{\mathcal{N} \circ \mathcal{U}(g)} - \Phi^{\mathcal{V}(g) \circ \mathcal{N}} \right\|_2^2 &= \frac{2}{d^2} \text{Tr}[\text{SWAP}(\mathcal{N} \otimes \mathcal{N})(\text{SWAP})] \\ &- \frac{2}{d^2} \text{Tr} \left[\text{SWAP} \left(\frac{1}{|G|} \sum_{g \in G} (\mathcal{V}(g) \circ \mathcal{N}) \otimes (\mathcal{N} \circ \mathcal{U}(g)) \right) (\text{SWAP}) \right], \end{aligned} \quad (80)$$

where the equality follows from essentially the same proof given for Lemma 3. Then we can again make use of Algorithm 3, in a similar fashion as discussed around (78), in order to estimate the asymmetry measure above.

3.4 Testing symmetries of Lindbladians

In this section, we apply the symmetry testing algorithm from Section 3.3 to the task of measuring the symmetry of a Lindbladian \mathcal{L} , as defined in (11). Given that the channel realized by the master equation in (11) is $e^{\mathcal{L}t}$, our basic idea is to test for symmetry of this channel by means of the algorithm from Section 3.3. As discussed previously, this amounts to estimating the two terms in (77) and (78) using Algorithm 3, but with the replacement $\mathcal{N} \rightarrow e^{\mathcal{L}t}$, and combining the estimates according to (63). The result is to form an estimate of the following asymmetry measure:

$$a(\mathcal{L}, t, \{\mathcal{U}(g)\}_{g \in G}) := \frac{1}{|G|} \sum_{g \in G} \left\| (\text{id} \otimes [\mathcal{U}(g), e^{\mathcal{L}t}]) (\Phi^d) \right\|_2^2, \quad (81)$$

In order to do so, we require a means by which the channel $e^{\mathcal{L}t}$ can be realized or simulated. We can accomplish the latter by employing one of several quantum algorithms for simulating Lindbladian evolutions [9, 13, 36, 60, 65] (see [55] for a review).

The basic condition for symmetry of a Lindbladian \mathcal{L} with respect to a unitary channel representation is as follows [30, 32, 31]:

$$\mathcal{L} \circ \mathcal{U}(g) = \mathcal{U}(g) \circ \mathcal{L} \quad \forall g \in G. \quad (82)$$

An alternative definition for symmetry of a Lindbladian \mathcal{L} with respect to a unitary channel representation $\{\mathcal{U}(g)\}_{g \in G}$ is similar to what we defined in (7)–(8), for channel symmetry [30, 32, 31]:

$$e^{\mathcal{L}t} \circ \mathcal{U}(g) = \mathcal{U}(g) \circ e^{\mathcal{L}t} \quad \forall t \in \mathbb{R}, g \in G. \quad (83)$$

In the following proposition, we recall the well known fact that these two definitions are actually equivalent:

Proposition 1 *The symmetry condition in (83) holds if and only if it holds for the Lindbladian \mathcal{L} , so that*

Proof. Suppose that (83) holds. We then find that

$$\left. \frac{\partial}{\partial t} (e^{\mathcal{L}t} \circ \mathcal{U}(g)) \right|_{t=0} = \left. \frac{\partial}{\partial t} (\mathcal{U}(g) \circ e^{\mathcal{L}t}) \right|_{t=0}. \quad (84)$$

The left-hand side then evaluates to $\mathcal{L} \circ \mathcal{U}(g)$ and the right-hand side to $\mathcal{U}(g) \circ \mathcal{L}$, concluding the proof of the if-part of the proposition. To see the other implication (the only-if part), suppose that (82) holds. Then

$$e^{\mathcal{L}t} \circ \mathcal{U}(g) = \sum_{\ell=0}^{\infty} \frac{(\mathcal{L}^\ell \circ \mathcal{U}(g)) t^\ell}{\ell!} = \sum_{\ell=0}^{\infty} \frac{(\mathcal{U}(g) \circ \mathcal{L}^\ell) t^\ell}{\ell!} = \mathcal{U}(g) \circ e^{\mathcal{L}t}, \quad (85)$$

where the second equality follows from repeated application of (82). ■

In fact, the main finding of [30] establishes a much stronger result: the symmetry condition in (82) is equivalent to the existence of a representation of \mathcal{L} of the form in (11), such that the completely positive map $(\cdot) \rightarrow \sum_k L_k(\cdot) L_k^\dagger$ is covariant with respect to $\{\mathcal{U}(g)\}_{g \in G}$ and $[U(g), H] = 0$ for all $g \in G$.

For small t , we perform a Taylor expansion of the Lindbladian term contained in the asymmetry measure as defined in (81), in order to elucidate a relation between approximate symmetry of the channel $e^{\mathcal{L}t}$ and the Lindbladian \mathcal{L} :

$$\frac{1}{|G|} \sum_{g \in G} \left\| (\text{id} \otimes [\mathcal{U}(g), e^{\mathcal{L}t}]) (\Phi^d) \right\|_2^2 \quad (86)$$

$$= \frac{1}{|G|} \sum_{g \in G} \left\| (\text{id} \otimes [\mathcal{U}(g), \text{id} + \mathcal{L}t + O(t^2)]) (\Phi^d) \right\|_2^2 \quad (87)$$

$$= \frac{1}{|G|} \sum_{g \in G} \left\| (\text{id} \otimes ([\mathcal{U}(g), \text{id}] + [\mathcal{U}(g), \mathcal{L}t] + [\mathcal{U}(g), O(t^2)])) (\Phi^d) \right\|_2^2 \quad (88)$$

$$= \frac{1}{|G|} \sum_{g \in G} \left\| (\text{id} \otimes ([\mathcal{U}(g), \mathcal{L}]t + [\mathcal{U}(g), O(t^2)])) (\Phi^d) \right\|_2^2 \quad (89)$$

$$= \frac{t^2}{|G|} \sum_{g \in G} \left\| (\text{id} \otimes [\mathcal{U}(g), \mathcal{L}]) (\Phi^d) \right\|_2^2 + O(t^3). \quad (90)$$

4 Simulations

In this section, we first describe two examples of open quantum systems, namely, the amplitude damping channel and a two-qubit spin chain. We subsequently present simulation results obtained from Qiskit implementations of the aforementioned systems, wherein we test them for symmetry with respect to the finite discrete group \mathbb{Z}_2 .¹

In the case of the amplitude damping channel, we use the algorithm discussed around (77)–(78) to estimate the asymmetry measure in (63) and then plot the same as a function of Γt , where Γ represents the rate of decay per unit time and t denotes time. We find that, for all values of Γt , when testing for Z symmetry (i.e., when our chosen unitary group representation for \mathbb{Z}_2 is $\{U(g)\}_{g \in \mathbb{Z}_2} = \{I, Z\}$), the asymmetry measure is approximately equal to zero with accuracy $\epsilon = 0.01$. On the other hand, we find that the X asymmetry measure diverges from zero with increasing values of Γt , which is consistent with the well known fact that the amplitude damping channel is not symmetric with respect to the representation $\{I, X\}$. Later in this section, we show that it varies with Γt as $\frac{1}{2} (1 - e^{-\Gamma t})^2$, which is consistent with our simulation results.

Similarly, we test a two-qubit spin-chain system for SWAP, $Z_1 Z_2$, and $X_1 X_2$ symmetries. We find symmetry to be preserved in the first two cases, wherein the corresponding asymmetry measures are found to be equal to zero. In the case of the $X_1 X_2$ symmetry test, however, we find that symmetry is broken. Later in this section, we derive the precise formula according to which the $X_1 X_2$ asymmetry measure is found to depend on Γ , t , and J . Both of the aforementioned examples are discussed in more detail in the subsequent subsections, along with the obtained simulation results and the methods whereby the simulations were performed.

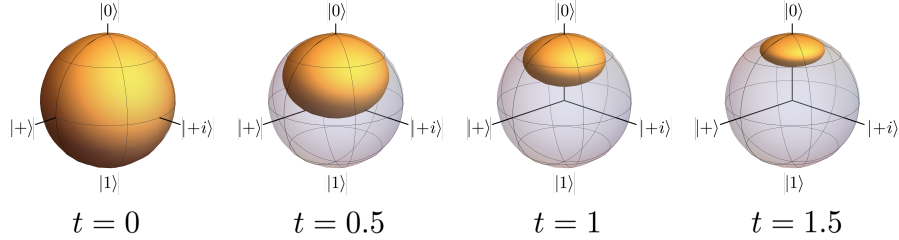


Figure 4: Illustration of the action of the $\Gamma = 1$ amplitude damping channel on the Bloch sphere over time. All states decay exponentially fast to $|0\rangle$.

4.1 Amplitude damping channel

The amplitude damping channel is a quantum channel that models loss of energy from a system to its environment. This can be used to describe open quantum systems that interact with their environment via processes such as spontaneous emission of a single photon from a two-level atomic system.

Continuous-time amplitude damping is generated by a Lindbladian using the raising operator $\sigma^+ := (X + iY)/2$ as a jump operator:

$$\mathcal{L}(\rho) = \Gamma \left(\sigma^+ \rho \sigma^- - \frac{1}{2} \{ \sigma^- \sigma^+, \rho \} \right), \quad (91)$$

where $\Gamma \geq 0$ represents the rate of $|1\rangle \rightarrow |0\rangle$ decay per unit time and $\sigma^- := (\sigma^+)^\dagger = (X - iY)/2$. We can obtain the superoperator $e^{\mathcal{L}t}$ representing time evolution under this Lindbladian for a time t by mapping Hilbert space operators to Liouville–Fock superoperators under the rule

$$A\rho B \mapsto (B^\top \otimes A)|\rho\rangle\rangle, \quad (92)$$

where A and B are Hilbert space operators, and $|\rho\rangle\rangle$ is the “vectorized” version of the density operator, formed by stacking the columns of ρ . Applying this to the Lindbladian yields

$$\mathcal{L}(\rho) = \Gamma \left(\sigma^+ \rho \sigma^- - \frac{1}{2} \{ \sigma^- \sigma^+, \rho \} \right) \quad (93)$$

$$\mapsto L|\rho\rangle\rangle := \Gamma \left(\sigma^+ \otimes \sigma^+ - \frac{1}{2} I \otimes (\sigma^- \sigma^+) - \frac{1}{2} (\sigma^- \sigma^+) \otimes I \right) |\rho\rangle\rangle, \quad (94)$$

¹All code used to run simulations, generate plots, and perform proof-related calculations is available at <https://github.com/radulaski/SymmetryTestingQuantumAlgorithms>.

so that the time evolution superoperator corresponds to

$$e^{Lt} = \exp \begin{pmatrix} 0 & 0 & 0 & \Gamma t \\ 0 & -\frac{\Gamma t}{2} & 0 & 0 \\ 0 & 0 & -\frac{\Gamma t}{2} & 0 \\ 0 & 0 & 0 & -\Gamma t \end{pmatrix} = \begin{pmatrix} 1 & 0 & 0 & 1 - e^{-\Gamma t} \\ 0 & e^{-\Gamma t/2} & 0 & 0 \\ 0 & 0 & e^{-\Gamma t/2} & 0 \\ 0 & 0 & 0 & e^{-\Gamma t} \end{pmatrix}. \quad (95)$$

The action of this matrix on a vectorized density matrix is

$$e^{Lt}|\rho\rangle\rangle = e^{Lt} \begin{pmatrix} \rho_{00} \\ \rho_{10} \\ \rho_{01} \\ \rho_{11} \end{pmatrix} = \begin{pmatrix} \rho_{00} + (1 - e^{-\Gamma t})\rho_{11} \\ e^{-\Gamma t/2}\rho_{10} \\ e^{-\Gamma t/2}\rho_{01} \\ e^{-\Gamma t}\rho_{11} \end{pmatrix}. \quad (96)$$

De-vectorizing the above, we find that

$$e^{\mathcal{L}t}(\rho) = \begin{pmatrix} \rho_{00} + (1 - e^{-\Gamma t})\rho_{11} & e^{-\Gamma t/2}\rho_{01} \\ e^{-\Gamma t/2}\rho_{10} & e^{-\Gamma t}\rho_{11} \end{pmatrix}. \quad (97)$$

It is well known that the time-independent amplitude damping channel \mathcal{D}_γ for a probability of decay γ can be represented by Kraus operators as

$$K_0 := \begin{pmatrix} 1 & 0 \\ 0 & \sqrt{1-\gamma} \end{pmatrix}, \quad K_1 := \begin{pmatrix} 0 & \sqrt{\gamma} \\ 0 & 0 \end{pmatrix}, \quad (98)$$

so that

$$\mathcal{D}_\gamma(\rho) = K_0\rho K_0^\dagger + K_1\rho K_1^\dagger = \begin{pmatrix} \rho_{00} + \gamma\rho_{11} & \sqrt{1-\gamma}\rho_{01} \\ \sqrt{1-\gamma}\rho_{10} & (1-\gamma)\rho_{11} \end{pmatrix}. \quad (99)$$

The equivalence of the two representations of the amplitude damping channel in (97) and (99) shows that $\gamma = 1 - e^{-\Gamma t}$.

4.1.1 Dependence of X asymmetry measure on Γt

Proposition 2 *For the amplitude damping channel in (97), the X asymmetry measure defined from (81) is given by*

$$a(\mathcal{L}, t, \{I, X\}) = \frac{1}{2}(1 - e^{-\Gamma t})^2, \quad (100)$$

where X is the σ_X Pauli matrix.

Proof. Let us consider two channels, denoted by \mathcal{D}_γ and \mathcal{X} . \mathcal{D}_γ is the amplitude damping channel, where γ denotes the probability of decay. Its action on a density matrix ρ is defined as in (99). The action of \mathcal{X} is defined as $\mathcal{X}(\rho) = X\rho X^\dagger$. Using these definitions, we calculate the actions of these channels on the elementary matrices $\{|i\rangle\langle j|\}_{i,j \in \{0,1\}}$ as follows:

$\mathcal{D}_\gamma(0\rangle\langle 0) = 0\rangle\langle 0 $	$\mathcal{X}(0\rangle\langle 0) = 1\rangle\langle 1 $
$\mathcal{D}_\gamma(0\rangle\langle 1) = \sqrt{1-\gamma} 0\rangle\langle 1 $	$\mathcal{X}(0\rangle\langle 1) = 1\rangle\langle 0 $
$\mathcal{D}_\gamma(1\rangle\langle 0) = \sqrt{1-\gamma} 1\rangle\langle 0 $	$\mathcal{X}(1\rangle\langle 0) = 0\rangle\langle 1 $
$\mathcal{D}_\gamma(1\rangle\langle 1) = \gamma 0\rangle\langle 0 + (1-\gamma) 1\rangle\langle 1 $	$\mathcal{X}(1\rangle\langle 1) = 0\rangle\langle 0 $

Next, we define two channels $\{\mathcal{N}, \mathcal{M}\}$, as follows:

$$\mathcal{N} := \mathcal{X} \circ \mathcal{D}_\gamma, \quad \mathcal{M} := \mathcal{D}_\gamma \circ \mathcal{X}. \quad (101)$$

The actions of the above defined channels with respect to a density matrix ρ are given by $\mathcal{N}(\rho) = \mathcal{X}(\mathcal{D}_\gamma(\rho))$ and $\mathcal{M}(\rho) = \mathcal{D}_\gamma(\mathcal{X}(\rho))$. Again, we may use the above definitions to calculate the following actions:

$\mathcal{N}(0\rangle\langle 0) = 1\rangle\langle 1 $	$\mathcal{M}(0\rangle\langle 0) = \gamma 0\rangle\langle 0 + (1-\gamma) 1\rangle\langle 1 $
$\mathcal{N}(0\rangle\langle 1) = \sqrt{1-\gamma} 1\rangle\langle 0 $	$\mathcal{M}(0\rangle\langle 1) = \sqrt{1-\gamma} 1\rangle\langle 0 $
$\mathcal{N}(1\rangle\langle 0) = \sqrt{1-\gamma} 0\rangle\langle 1 $	$\mathcal{M}(1\rangle\langle 0) = \sqrt{1-\gamma} 0\rangle\langle 1 $
$\mathcal{N}(1\rangle\langle 1) = (1-\gamma) 0\rangle\langle 0 + \gamma 1\rangle\langle 1 $	$\mathcal{M}(1\rangle\langle 1) = 0\rangle\langle 0 $

Let us consider a general unitary representation of the finite discrete group \mathbb{Z}_2 , given by $\{U(g)\}_{g \in \mathbb{Z}_2} = \{I, W\}$, where I is the two-qubit identity operator, and W is some two-qubit unitary operator satisfying $W^2 = I$. Furthermore, let the unitary channels constituting $\{U(g)\}_{g \in \mathbb{Z}_2}$ and corresponding to I and W be denoted by \mathcal{I} and \mathcal{W} respectively. We may then define the asymmetry measure given in (81), with respect to some Lindbladian channel $e^{\mathcal{L}t}$ and the aforementioned unitary representation $\{I, W\}$, as follows:

$$\begin{aligned} & a(\mathcal{L}, t, \{I, W\}) \\ &= \frac{1}{2} \sum_{g \in \mathbb{Z}_2} \|(\text{id} \otimes [U(g), e^{\mathcal{L}t}]) (\Phi^2)\|_2^2 \end{aligned} \quad (102)$$

$$= \frac{1}{2} \left(\|(\text{id} \otimes [\mathcal{I}, e^{\mathcal{L}t}]) (\Phi^2)\|_2^2 + \|(\text{id} \otimes [\mathcal{W}, e^{\mathcal{L}t}]) (\Phi^2)\|_2^2 \right) \quad (103)$$

$$= \frac{1}{2} \left(\|(\text{id} \otimes [\mathcal{W}, e^{\mathcal{L}t}]) (\Phi^2)\|_2^2 \right) \quad (104)$$

$$= \frac{1}{2} \left(\left\| \Phi^{\mathcal{W} \circ e^{\mathcal{L}t}} - \Phi^{e^{\mathcal{L}t} \circ \mathcal{W}} \right\|_2^2 \right) \quad (105)$$

Now, in order to compute our desired asymmetry measure, we simply substitute the Lindbladian channel $e^{\mathcal{L}t}$ by \mathcal{D}_γ , and the unitary channel \mathcal{W} by \mathcal{X} . We then have

$$\begin{aligned} a(\mathcal{L}, t, \{I, X\}) &= \frac{1}{2} \left(\left\| \Phi^{\mathcal{X} \circ \mathcal{D}_\gamma} - \Phi^{\mathcal{D}_\gamma \circ \mathcal{X}} \right\|_2^2 \right) \end{aligned} \quad (106)$$

$$= \frac{1}{2} \left(\left\| \Phi^{\mathcal{N}} - \Phi^{\mathcal{M}} \right\|_2^2 \right) \quad (107)$$

$$= \frac{1}{2} \left(\text{Tr}[(\Phi^{\mathcal{N}})^2] + \text{Tr}[(\Phi^{\mathcal{M}})^2] - 2 \text{Tr}[\Phi^{\mathcal{N}} \Phi^{\mathcal{M}}] \right) \quad (108)$$

$$= \text{Tr}[(\Phi^{\mathcal{D}_\gamma})^2] - \text{Tr}[\Phi^{\mathcal{N}} \Phi^{\mathcal{M}}], \quad (109)$$

where the last line follows because $\text{Tr}[(\Phi^{\mathcal{D}_\gamma})^2] = \text{Tr}[(\Phi^{\mathcal{N}})^2] = \text{Tr}[(\Phi^{\mathcal{M}})^2]$, which in turn follows from (67). Additionally, from (48), we know that for any two quantum channels \mathcal{N} and \mathcal{M} , the overlap term $\text{Tr}[\Phi^{\mathcal{N}} \Phi^{\mathcal{M}}]$ may be expressed as

$$\text{Tr}[\Phi^{\mathcal{N}} \Phi^{\mathcal{M}}] = \frac{1}{d^2} \sum_{i,j} \text{Tr}[\mathcal{N}(|i\rangle\langle j|) \mathcal{M}(|j\rangle\langle i|)]. \quad (110)$$

Using the above formula, we find that

$ i\rangle\langle j $	$\text{Tr}[\mathcal{D}_\gamma(i\rangle\langle j) \mathcal{D}_\gamma(j\rangle\langle i)]$	$\text{Tr}[\mathcal{N}(i\rangle\langle j) \mathcal{M}(j\rangle\langle i)]$
$ 0\rangle\langle 0 $	1	$1 - \gamma$
$ 0\rangle\langle 1 $	$1 - \gamma$	$1 - \gamma$
$ 1\rangle\langle 0 $	$1 - \gamma$	$1 - \gamma$
$ 1\rangle\langle 1 $	$\gamma^2 + (1 - \gamma)^2$	$1 - \gamma$

We can now calculate each of the two terms in (109). For $\text{Tr}[(\Phi^{\mathcal{D}_\gamma})^2]$, we

have:

$$\mathrm{Tr}\left[(\Phi^{\mathcal{D}_\gamma})^2\right] = \frac{1}{d^2} \sum_{i,j} \mathrm{Tr}[\mathcal{D}_\gamma(|i\rangle\langle j|)\mathcal{D}_\gamma(|j\rangle\langle i|)] \quad (111)$$

$$= \frac{1}{4} [1 + 1 - \gamma + 1 - \gamma + \gamma^2 + (1 - \gamma)^2] \quad (112)$$

$$= \frac{1}{2} [\gamma^2 - 2\gamma + 2]. \quad (113)$$

For $\mathrm{Tr}[\Phi^{\mathcal{N}}\Phi^{\mathcal{M}}]$, we have

$$\mathrm{Tr}[\Phi^{\mathcal{N}}\Phi^{\mathcal{M}}] = \frac{1}{d^2} \sum_{i,j} \mathrm{Tr}[\mathcal{N}(|i\rangle\langle j|)\mathcal{M}(|j\rangle\langle i|)] \quad (114)$$

$$= \frac{1}{4} [1 - \gamma + 1 - \gamma + 1 - \gamma + 1 - \gamma] \quad (115)$$

$$= 1 - \gamma. \quad (116)$$

Plugging the above obtained results into (109), and recalling the identification $\gamma = 1 - e^{-\Gamma t}$ made in the previous subsection, we conclude that

$$a(\mathcal{L}, t, \{I, X\}) = \frac{\gamma^2}{2} = \frac{(1 - e^{-\Gamma t})^2}{2}. \quad (117)$$

We have thus computed X asymmetry measure both as a function of the overall probability of decay γ , as well as the probability of decay per unit time, Γ , and time t . ■

We note here that it is interesting to compare the value in Proposition 2 with Proposition IV.2 of [44]. The latter proposition evaluated an asymmetry measure of the amplitude damping channel in terms of the normalized diamond distance, which is another method for measuring the distance between two quantum channels. Therein, a value of $\frac{1}{2} (1 - e^{-\Gamma t})$ was reported. Thus, both measures increase with increasing Γt , as would be expected for any X -asymmetry measure for the amplitude damping channel; however, they increase differently, due to the differing choices of measures.

4.1.2 Amplitude damping channel simulation results

We used Qiskit's `QasmSimulator` to simulate the execution of Algorithm 3 on an idealized quantum processor in order to calculate the X and Z symmetries of the amplitude damping channel. We implement the (non-unitary)

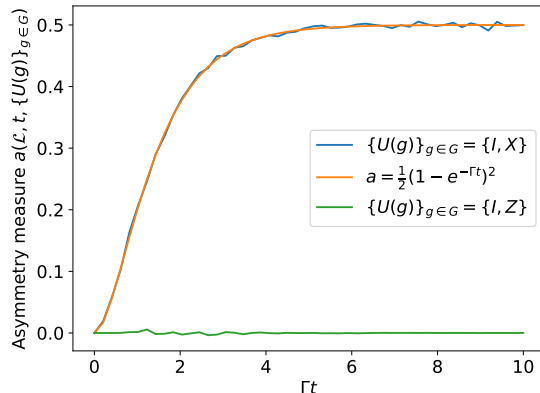


Figure 5: Simulated results of applying Algorithm 3 to measure X and Z asymmetries of the single-qubit amplitude damping channel, using Qiskit’s noiseless `QasmSimulator`. The simulation shows that the system maintains Z symmetry for any value of amplitude dissipation Γt , while X symmetry is lost for $\Gamma t > 0$. The measure of X asymmetry closely matches the analytical expression $\frac{1}{2} (1 - e^{-\Gamma t})^2$ in the absence of noise. All simulations were run with a total number of shots determined by the Hoeffding inequality (Theorem 1) with $\epsilon, \delta = 0.01$.

amplitude damping channel \mathcal{D}_γ by means of a unitary extension D_γ , which requires an additional “environment” qubit:

$$D_\gamma = \begin{pmatrix} 0 & \sqrt{\gamma} & -\sqrt{1-\gamma} & 0 \\ 0 & 0 & 0 & 1 \\ 1 & 0 & 0 & 0 \\ 0 & \sqrt{1-\gamma} & \sqrt{\gamma} & 0 \end{pmatrix}, \quad (118)$$

so that

$$\mathcal{D}_\gamma(\rho) = \text{Tr}_1 \left[D_\gamma (|0\rangle\langle 0| \otimes \rho) D_\gamma^\dagger \right]. \quad (119)$$

Using (118) to implement the amplitude damping channel, we constructed Algorithm 3 in Qiskit and used it to measure the X and Z asymmetries of the channel. We executed the algorithm on Qiskit’s `QasmSimulator`, which emulates an idealized quantum processor with no decoherence. The results, plotted in Figure 5, show the expected Z symmetry and X asymmetry, in agreement with the analytical expression.

We also executed the same symmetry tests using Qiskit’s `FakeLima` backend, which provides a depolarizing noise model with parameters estimated from a real quantum processor. These results are plotted in Figure 6. The

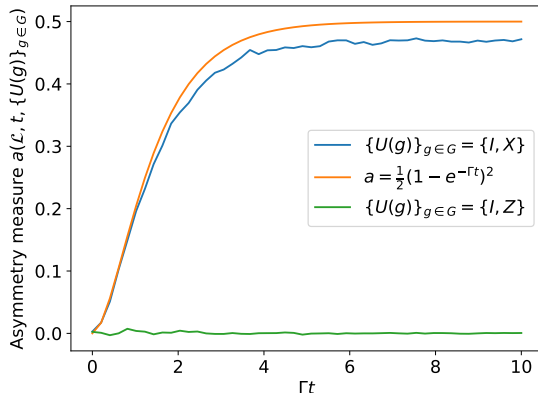


Figure 6: Simulated results of applying Algorithm 3 to measure X and Z symmetries of the single-qubit amplitude damping channel, using Qiskit’s FakeLima backend. The simulation shows that the system maintains Z symmetry for any value of amplitude dissipation Γt , while X symmetry is lost for $\Gamma t > 0$. The measure of X asymmetry deviates slightly from the analytical relationship $\frac{1}{2}(1 - e^{-\Gamma t})^2$ due to the simulated depolarizing noise. All simulations were run with a total number of shots determined by the Hoeffding inequality (Theorem 1) with $\epsilon, \delta = 0.01$.

Z asymmetry remains zero, while the X asymmetry shows a slight reduction relative to the analytical expression, which accords with the presence of depolarizing noise.

4.2 XX Spin chain

Systems of spin-1/2 particles with nearest-neighbor exchange interactions have been studied for nearly a century and are foundational models in the exploration of magnetism in condensed matter physics [45]. See Figure 7 for a visualization. In the context of quantum information, spin chains have been studied for potential applications to quantum state transfer. We consider an open XX Heisenberg spin chain consisting of two particles, each of which is subject to amplitude damping dissipation. This system is governed by the Lindblad master equation

$$\mathcal{L}(\rho) = -i[H, \rho] + \sum_{i=1}^2 \mathcal{L}_i(\rho), \quad (120)$$

where the Hamiltonian H is given by

$$H = J(X_1 X_2 + Y_1 Y_2), \quad (121)$$

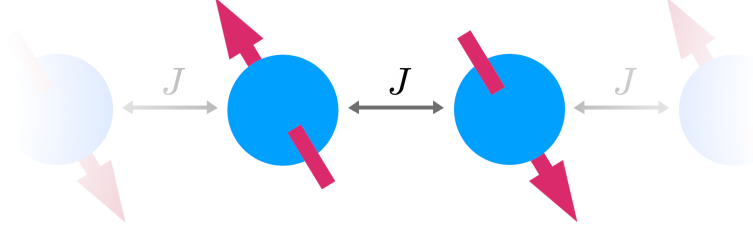


Figure 7: Visualization of a spin chain. Each particle’s spin couples to that of its neighbors at a rate J . We use Algorithm 3 to examine various symmetries of a two-particle spin chain.

and each \mathcal{L}_i term acts on qubit i and is an amplitude dissipation Lindbladian, as defined in (91). In the above, $J \geq 0$ represents the rate at which excitations hop from one site in the chain to the other.

4.2.1 Spin-chain asymmetries as a function of Γt

Since amplitude damping dissipation is a longitudinal interaction, this system is manifestly $Z_1 Z_2$ -symmetric for any amount of damping Γt . Conversely, the $X_1 X_2$ symmetry of the Hamiltonian is broken by nonzero energy dissipation. Finally, the interactions between the two halves of the system are symmetrical, and so the system is manifestly symmetric under a SWAP of the two particles. Here we use direct calculation of (81) to show the $Z_1 Z_2$ and SWAP symmetries, and calculate the measure of $X_1 X_2$ asymmetry as a function of Γt .

Proposition 3 *For the open two-qubit XX spin chain defined in (120), the $Z_1 Z_2$, SWAP, and $X_1 X_2$ asymmetry measures defined from (81) are given by*

$$a(\mathcal{L}, t, \{I, Z_1 Z_2\}) = 0, \quad a(\mathcal{L}, t, \{I, \text{SWAP}\}) = 0, \quad (122)$$

and

$$a(\mathcal{L}, t, \{I, X_1 X_2\}) = \frac{e^{-2t\Gamma} (-t^2\Gamma^2 \cos(4J) - 16J^2 \cosh(t\Gamma) + (16J^2 + t^2\Gamma^2) \cosh(2t\Gamma))}{32J^2 + 2t^2\Gamma^2}. \quad (123)$$

Proof. We calculate the Choi states in (105) in terms of the superoperator representations of the channels \mathcal{W} and $e^{\mathcal{L}t}$. Applying the prescription (92) to the terms of the Lindbladian (120) and operator W , we obtain

$$W \mapsto W^\top \otimes W, \quad (124)$$

and

$$\begin{aligned} \mathcal{L} \mapsto & -i((I \otimes H) - (H^\top \otimes I)) \\ & + \sum_i \Gamma \left(\sigma_i^+ \otimes \sigma_i^+ - \frac{1}{2} I \otimes (\sigma_i^- \sigma_i^+) - \frac{1}{2} (\sigma_i^- \sigma_i^+) \otimes I \right). \end{aligned} \quad (125)$$

The latter is straightforwardly exponentiated to obtain a superoperator matrix form of $e^{\mathcal{L}t}$.

Applying these representations to (13), inserting these Choi states into (105) and simplifying with the aid of the computer algebra system Mathematica (code available with our arXiv post), for the three cases of interest $W \in \{Z_1 Z_2, \text{SWAP}, X_1 X_2\}$ we obtain the expressions given in the proposition. ■

4.2.2 Spin-chain simulation results

To emulate the dynamics described by (120) on a quantum processor as part of the algorithm discussed around (81), we must address two issues. First, the dissipative terms in \mathcal{L} must be replaced by unitary extensions acting on additional “environment” qubits, in order to make them implementable by unitary gates. Second, noncommuting terms in \mathcal{L} make it necessary to use Trotterization to implement $e^{\mathcal{L}t}$.

We Trotterize the Lindbladian following the prescription in [10, Proposition 2]:

$$e^{\mathcal{L}t} = \exp\left(t \sum_{i=1}^m \mathcal{L}_i\right) \approx \left(\prod_{i=1}^m e^{\mathcal{L}_i t/2N} \prod_{j=m}^1 e^{\mathcal{L}_j t/2N} \right)^N, \quad (126)$$

The specific ordering of terms in this product (forwards and then backwards) results in the first and second orders of the Taylor expansions of the left and right sides of (126) to agree exactly.

We note that the terms $-i[H_j, (\cdot)]$ arising from the Hamiltonian induce unitary evolution, and so can be implemented simply as $e^{-iH_j t}$. The two dissipative Lindblad terms can be implemented using D_γ , the unitary extension of the amplitude damping channel (118), provided that the environment qubit is reset to zero before each application of D_γ . Therefore, each Trotter step of the spin chain Lindbladian can be implemented using

$$\prod_{i=1}^m e^{\mathcal{L}_i t/2N} \mapsto e^{-iX_1 X_2 t/2N} e^{-iY_1 Y_2 t/2N} D_{1-e^{-\Gamma t/2N}}^1 D_{1-e^{-\Gamma t/2N}}^2, \quad (127)$$

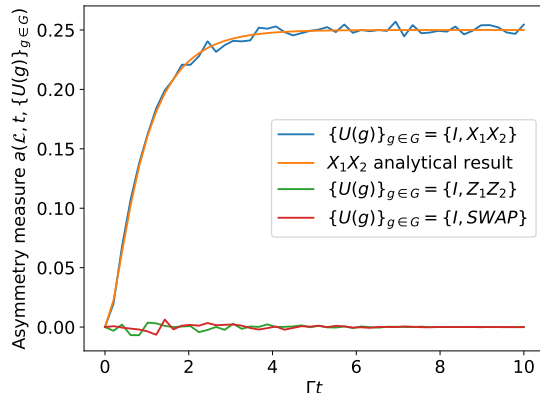


Figure 8: Simulation results for applying Algorithm 3 to the two-qubit spin chain using Qiskit’s noiseless `QasmSimulator`. We test the system for X_1X_2 , Z_1Z_2 , and SWAP symmetries. In the latter two cases, the system exhibits symmetry; the asymmetry measure deviates from zero only due to sampling error. In contrast, the system’s lack of X_1X_2 symmetry is evident for nonzero values of Γt , and the value of the asymmetry measure in this case agrees closely with the analytical result from (123).

$$\prod_{i=m}^1 e^{\mathcal{L}_i t/2N} \mapsto D_{1-e^{-\Gamma t/2N}}^2 D_{1-e^{-\Gamma t/2N}}^1 e^{-iY_1 Y_2 t/2N} e^{-iX_1 X_2 t/2N}. \quad (128)$$

This implementation is essentially the same as that presented in Figure 1 of [13], up to a Trotterization of the unitary dynamics, and reordering of the Trotter terms.

We used this formulation to implement Algorithm 3 in Qiskit. We then executed it on Qiskit’s `QasmSimulator` to test the 2-particle spin chain system for X_1X_2 , Z_1Z_2 , and SWAP symmetries, using a number of shots determined by Hoeffding inequality (Theorem 1) with $\epsilon, \delta = 0.01$. The resulting estimates of the asymmetry measure are plotted in Figure 8, where we can see that Z_1Z_2 and SWAP symmetries are maintained in the presence of amplitude damping, while X_1X_2 symmetry is broken to the degree specified in (123).

As in the case of our previous simulations of the amplitude damping channel, we also test our spin-chain system for symmetry in the presence of a depolarizing noise model. We do this, as before, by running our code using Qiskit’s `FakeLima` backend. Consistent with the nature of the noise model imported, we find in Figure 9 that the obtained plot of the X_1X_2 asymmetry

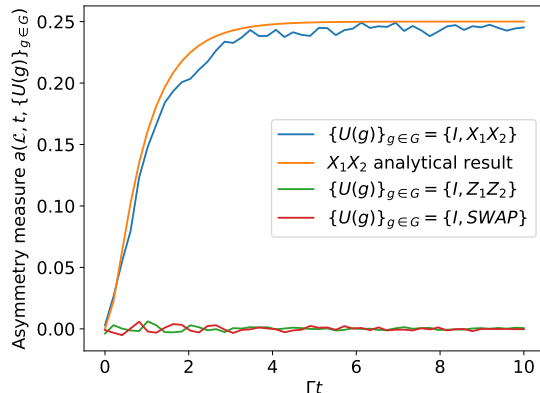


Figure 9: Simulation results for applying Algorithm 3 to the two-qubit spin chain using Qiskit’s FakeLima backend, which includes realistic depolarizing noise. We test the system for X_1X_2 , Z_1Z_2 , and SWAP symmetries. As in the noiseless simulation (Figure 8), we verify Z_1Z_2 and SWAP symmetries, and X_1X_2 asymmetry, although the latter deviates from its analytical expression slightly due to the depolarizing noise.

measure is slightly reduced with respect to the analytical expression as given in (123), while both Z_1Z_2 and SWAP symmetries appear to be preserved.

5 Measurements: Estimating Hilbert–Schmidt distance and testing symmetries

In this section, we consider a special case of the developments in Sections 3.2 and 3.3, when the channels of interest are measurement channels, meaning that they can be written in the following form:

$$\mathcal{N}(\omega) = \sum_x \text{Tr}[N_x \omega] |x\rangle\langle x|, \quad (129)$$

where ω is an input state being measured, $\{N_x\}_x$ is a positive operator-valued measure (POVM) (satisfying $N_x \geq 0$ for all x and $\sum_x N_x = I$), and $\{|x\rangle\}_x$ is an orthonormal basis, such that the classical state $|x\rangle\langle x|$ encodes the measurement outcome.

We begin by providing an algorithm for estimating the Hilbert–Schmidt distance of the Choi states of two measurement channels (Section 5.1). In principle, since measurement channels are a particular kind of channel, one

could simply apply Algorithm 3 for this task. However, our developments below demonstrate that this algorithm can be significantly simplified in this case, as a consequence of the channel outputs being classical.

After that, we then recall the definition of covariance symmetry of measurement channels and devise an algorithm for testing this symmetry (Section 5.2). We note that this kind of symmetry is a special case of the channel symmetry mentioned in Remark 1.

5.1 Estimating the Hilbert–Schmidt distance of the Choi states of measurement channels

We are interested in estimating the Hilbert–Schmidt distance between the Choi states of two measurement channels, defined as in (130) below. Since measurement channels are indeed channels, the expression for the Hilbert–Schmidt distance is precisely the same as that given in (43).

We begin our development with the following lemma, which shows how the various terms in (43) simplify when \mathcal{N} and \mathcal{M} are measurement channels.

Lemma 4 *Let \mathcal{N} and \mathcal{M} be measurement channels with d -dimensional inputs, so that*

$$\mathcal{N}(\omega) = \sum_x \text{Tr}[N_x \omega] |x\rangle\langle x|, \quad \mathcal{M}(\omega) = \sum_x \text{Tr}[M_x \omega] |x\rangle\langle x|, \quad (130)$$

where $\{N_x\}_x$ and $\{M_x\}_x$ are POVMs. Then

$$\text{Tr}[\Phi^{\mathcal{N}} \Phi^{\mathcal{M}}] = \frac{1}{d^2} \sum_{x,y} \delta_{x,y} \text{Tr}[(N_x \otimes M_y) (\text{SWAP})]. \quad (131)$$

Proof. Recalling (45)–(48), we find that

$$\begin{aligned} & \text{Tr}[\Phi^{\mathcal{N}} \Phi^{\mathcal{M}}] \\ &= \frac{1}{d^2} \sum_{i,j} \text{Tr}[\mathcal{N}(|i\rangle\langle j|) \mathcal{M}(|j\rangle\langle i|)] \end{aligned} \quad (132)$$

$$= \frac{1}{d^2} \sum_{i,j} \text{Tr} \left[\left(\sum_x \text{Tr}[N_x |i\rangle\langle j|] |x\rangle\langle x| \right) \left(\sum_y \text{Tr}[M_y |j\rangle\langle i|] |y\rangle\langle y| \right) \right] \quad (133)$$

$$= \frac{1}{d^2} \sum_{i,j,x,y} \text{Tr}[N_x |i\rangle\langle j|] \text{Tr}[M_y |j\rangle\langle i|] \text{Tr}[|x\rangle\langle x| |y\rangle\langle y|] \quad (134)$$

$$= \frac{1}{d^2} \sum_{i,j,x,y} \delta_{x,y} \text{Tr}[N_x |i\rangle\langle j|] \text{Tr}[M_y |j\rangle\langle i|] \quad (135)$$

$$= \frac{1}{d^2} \sum_{x,y} \delta_{x,y} \text{Tr}[(N_x \otimes M_y) (\text{SWAP})], \quad (136)$$

concluding the proof. ■

If the inputs to the channels are n -qubit states and the outputs are m -bit strings \vec{x} and \vec{y} , then following the development and notation from (51)–(56), we can write

$$\begin{aligned} \text{Tr}[\Phi^{\mathcal{N}} \Phi^{\mathcal{M}}] &= \frac{1}{2^{2n}} \sum_{\vec{x}, \vec{y}} \delta_{\vec{x}, \vec{y}} \text{Tr}[(N_{\vec{x}} \otimes M_{\vec{y}}) (\text{SWAP}^{(n)})] \\ &= \frac{1}{2^{2n}} \sum_{\vec{x}, \vec{y} \in \{0,1\}^m} \sum_{\vec{k}, \vec{\ell} \in \{0,1\}^n} \delta_{\vec{x}, \vec{y}} (-1)^{\vec{k} \cdot \vec{\ell}} \text{Tr}[(N_{\vec{x}} \otimes M_{\vec{y}}) (\Phi^{\vec{k}\vec{\ell}})]. \end{aligned} \quad (137)$$

$$(138)$$

Now, by setting $Z \equiv (\vec{X}, \vec{Y}, \vec{K}, \vec{L})$ to be a multi-indexed random variable taking the value $\delta_{\vec{x}, \vec{y}} (-1)^{\vec{k} \cdot \vec{\ell}}$ with probability

$$p(\vec{x}, \vec{y}, \vec{k}, \vec{\ell}) = p(\vec{x}, \vec{y} | \vec{k}, \vec{\ell}) p(\vec{k}, \vec{\ell}), \quad (139)$$

where

$$p(\vec{k}, \vec{\ell}) = \frac{1}{2^{2n}}, \quad (140)$$

$$p(\vec{x}, \vec{y} | \vec{k}, \vec{\ell}) = \text{Tr}[(N_{\vec{x}} \otimes M_{\vec{y}}) (\Phi^{\vec{k}\vec{\ell}})], \quad (141)$$

we find from the above that its expectation is given by

$$\mathbb{E}[Z] = \text{Tr}[\Phi^{\mathcal{N}} \Phi^{\mathcal{M}}]. \quad (142)$$

This leads to the following quantum algorithm for estimating $\text{Tr}[\Phi^{\mathcal{N}} \Phi^{\mathcal{M}}]$, within additive error ε and with success probability not smaller than $1 - \delta$, where $\varepsilon > 0$ and $\delta \in (0, 1)$.

Algorithm 4 *Given are quantum circuits to implement the measurement channels \mathcal{N} and \mathcal{M} .*

1. Fix $\varepsilon > 0$ and $\delta \in (0, 1)$. Set $T \geq \frac{2}{\varepsilon^2} \ln(\frac{2}{\delta})$ and set $t = 1$.
2. Generate the bit vectors \vec{k} and $\vec{\ell}$ uniformly at random.
3. Prepare the Bell state $\Phi^{\vec{k}\vec{\ell}}$ on $2n$ qubits (using the ordering specified in (56)).

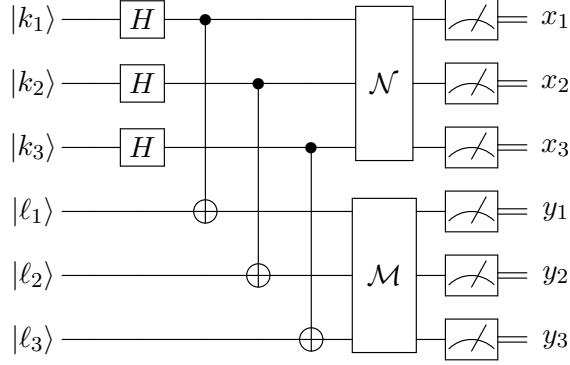


Figure 10: Depiction of the core quantum subroutine given in Steps 2.-4. of Algorithm 4, such that the measurement channels \mathcal{N} and \mathcal{M} have three-qubit inputs and three-bit outputs. This algorithm estimates the overlap $\text{Tr}[\Phi^{\mathcal{N}}\Phi^{\mathcal{M}}]$ of the Choi states of the measurement channels. In this example, the algorithm begins by preparing the classical state $|k_1, k_2, k_3, \ell_1, \ell_2, \ell_3\rangle$, where the values $k_1, k_2, k_3, \ell_1, \ell_2, \ell_3$ are chosen uniformly at random, followed by a sequence of controlled NOTs and Hadamards. Before the measurement channels are applied, the state is thus $|\Phi^{\vec{k}\vec{\ell}}\rangle$, as described in Algorithm 4. The measurement channels are then applied, leading to the classical bit string $x_1x_2x_3y_1y_2y_3$. In the diagram, we depict the realization of the measurement channels \mathcal{N} and \mathcal{M} as black boxes, but in a simulation of them, one might make use of additional environment qubits that are prepared and then discarded.

4. Apply the tensor-product measurement channel $\mathcal{N} \otimes \mathcal{M}$ (using the ordering specified after (56)), which leads to the measurement outcomes \vec{x} and \vec{y} .
5. Set $Y_t = \delta_{\vec{x}, \vec{y}} (-1)^{\vec{k} \cdot \vec{\ell}}$.
6. Increment t .
7. Repeat Steps 2.-6. until $t > T$ and then output $\bar{Y} := \frac{1}{T} \sum_{t=1}^T Y_t$ as an estimate of $\text{Tr}[\Phi^{\mathcal{N}}\Phi^{\mathcal{M}}]$.

Figure 10 depicts the core quantum subroutine of Algorithm 4. By the Hoeffding inequality (recalled as Theorem 1), we are guaranteed that the output of Algorithm 4 satisfies

$$\Pr[|\bar{Y} - \text{Tr}[\Phi^{\mathcal{N}}\Phi^{\mathcal{M}}]| \leq \varepsilon] \geq 1 - \delta, \quad (143)$$

due to the choice $T \geq \frac{2}{\varepsilon^2} \ln(\frac{2}{\delta})$.

By employing Algorithm 4 three times, we can thus estimate (43) for two measurement channels \mathcal{N} and \mathcal{M} within additive error ε and with success probability not smaller than $1 - \delta$, by using $O(\frac{1}{\varepsilon^2} \ln(\frac{1}{\delta}))$ samples of the measurement channels \mathcal{N} and \mathcal{M} .

5.2 Testing symmetries of measurement channels

A POVM $\{N_x\}_x$ is covariant if there exists a unitary representation $\{U(g)\}_{g \in G}$ of a group G such that

$$U(g)^\dagger N_x U(g) \in \{N_x\}_x \quad \forall g \in G, x. \quad (144)$$

Covariant POVMs have been studied previously [14, 34, 7, 15], and they appear in several applications, including state discrimination [38] and estimation [11]. Connecting to our previous notion of channel symmetry from Remark 1, a measurement channel \mathcal{N} is covariant if there exist unitary channel representations $\{U(g)\}_{g \in G}$ and $\{W(g)\}_{g \in G}$ such that

$$\mathcal{N} \circ U(g) = W(g) \circ \mathcal{N} \quad \forall g \in G. \quad (145)$$

Plugging into (129), the condition in (145) becomes

$$\sum_x \text{Tr}[U(g)^\dagger N_x U(g) \rho] |x\rangle\langle x| = \sum_x \text{Tr}[N_x \rho] W(g) |x\rangle\langle x| W(g)^\dagger \quad \forall g \in G. \quad (146)$$

Given that the output system is classical, we can restrict the unitary $W(g)$ to be a shift operator that realizes a permutation π_g of the classical letter x , so that

$$W(g) |x\rangle = |\pi_g(x)\rangle, \quad (147)$$

and thus (146) becomes

$$\sum_x \text{Tr}[U(g)^\dagger N_x U(g) \rho] |x\rangle\langle x|_X = \sum_x \text{Tr}[N_x \rho] |\pi_g(x)\rangle\langle \pi_g(x)|_X \quad (148)$$

$$= \sum_x \text{Tr}[N_{\pi_g^{-1}(x)} \rho] |x\rangle\langle x|_X. \quad (149)$$

Since this equation holds for every input state ρ , we conclude that the following condition holds for a covariant measurement channel:

$$U(g)^\dagger N_x U(g) = N_{\pi_g^{-1}(x)} \quad \forall g \in G, x, \quad (150)$$

coinciding with the definition given in (144).

We are interested in testing the covariance symmetry of the measurement channel \mathcal{N} , and we can do so by testing the following asymmetry measure:

$$\frac{1}{|G|} \sum_{g \in G} \left\| \Phi^{\mathcal{N} \circ \mathcal{U}(g)} - \Phi^{\mathcal{W}(g) \circ \mathcal{N}} \right\|_2^2, \quad (151)$$

related to the asymmetry measure from (62). By invoking Lemma 3, we find that

$$\begin{aligned} & \frac{1}{|G|} \sum_{g \in G} \left\| \Phi^{\mathcal{N} \circ \mathcal{U}(g)} - \Phi^{\mathcal{W}(g) \circ \mathcal{N}} \right\|_2^2 = \frac{2}{d^2} \text{Tr}[\text{SWAP}(\mathcal{N} \otimes \mathcal{N})(\text{SWAP})] \\ & - \frac{2}{d^2} \text{Tr} \left[\text{SWAP} \left(\frac{1}{|G|} \sum_{g \in G} (\mathcal{W}(g) \circ \mathcal{N}) \otimes (\mathcal{N} \circ \mathcal{U}(g)) \right) (\text{SWAP}) \right]. \end{aligned} \quad (152)$$

Now invoking Lemma 4, we conclude that

$$\text{Tr}[\text{SWAP}(\mathcal{N} \otimes \mathcal{N})(\text{SWAP})] = \sum_{x,y} \delta_{x,y} \text{Tr}[(N_x \otimes N_y)(\text{SWAP})], \quad (153)$$

and

$$\begin{aligned} & \text{Tr} \left[\text{SWAP} \left(\frac{1}{|G|} \sum_{g \in G} (\mathcal{W}(g) \circ \mathcal{N}) \otimes (\mathcal{N} \circ \mathcal{U}(g)) \right) (\text{SWAP}) \right] \\ & = \frac{1}{|G|} \sum_{g \in G} \sum_{x,y} \delta_{\pi_g(x),y} \text{Tr} \left[(N_x \otimes U^\dagger(g) N_y U(g)) (\text{SWAP}) \right]. \end{aligned} \quad (154)$$

The latter equality follows because $\mathcal{N} \circ \mathcal{U}(g)$ is a measurement channel with measurement operators $\{U^\dagger(g) N_x U(g)\}_x$ while $\mathcal{W}(g) \circ \mathcal{N}$ is a measurement channel with measurement operators $\{N_{\pi_g^{-1}(x)}\}_x$. As such, we can employ Algorithm 4 to estimate both terms in (153) and (154), and thus estimate (151) by subtracting them and multiplying the result by $\frac{2}{d^2}$. For estimating the latter term, in each step of the algorithm, we pick $g \in G$ uniformly at random, as before.

6 Conclusion and discussion

In this work, we proposed asymmetry measures for quantum states, channels, and measurements, as well as efficient quantum algorithms for estimating these measures. A key component of the algorithms for channels and

measurements are methods for efficiently estimating the overlap of their Choi states. We demonstrated the channel symmetry testing algorithm in two cases: the single-qubit amplitude damping channel and an open XX spin chain subject to amplitude dissipation. In both cases, we simulated our algorithm using Qiskit’s simulator and found excellent agreement with the analytical expression of the asymmetry measure. Finally, we discussed which near-term QPU architectures maximize the system size to be tested using the developed algorithms.

Prospects for implementing on near-term quantum hardware—

The developed quantum algorithms for symmetry testing can be readily implemented on near-term quantum hardware, as well as potentially guide the development of architectures for upcoming quantum testbeds. We have implemented the Lindbladian symmetry testing algorithm in such a way that the number of physical qubits in hardware is at least four times the number of qubits in the model. The depth of the circuit depends on the selection of Trotterization parameters, and for a specific quantum processing unit (QPU), these parameters should be selected within the hardware coherence limits.

Furthermore, the qubit connectivity has an important practical role in enabling implementation of the developed algorithms. Each of the algorithms requires the model to be mapped twice to physical qubits in what we will call subcircuits A and B (Figure 11). Entangling gates are applied to pairs of qubits in subcircuits A and B close to the beginning and/or the end of the algorithm, while the rest of the algorithm requires only local gates inside the subcircuits. This algorithmic split into two computing layers that are cross-connected only once or twice during the implementation of the symmetry testing algorithms lends itself well to upcoming QPU architectures on the IBM Quantum roadmap [23], Crossbill and Flamingo, for the purposes of maximizing the computable model size. These multi-chip processors are connected either with a smaller number of higher fidelity quantum gates implemented via short chip-to-chip connectors (Crossbill), or a larger number of slower and lower-fidelity quantum gates implemented via long-range couplers (Flamingo). In terms of symmetry testing algorithms where subcircuits A and B would be implemented on different chips, the Crossbill architecture would be suitable for models with a smaller number of qubits and deeper quantum algorithms, while the Flamingo architecture would be more suitable for larger systems that are either implemented via shallower circuits or are executed for algorithms that require only one time-step entanglement via the long-range connectors (SWAP test or measurement channel symmetry test).

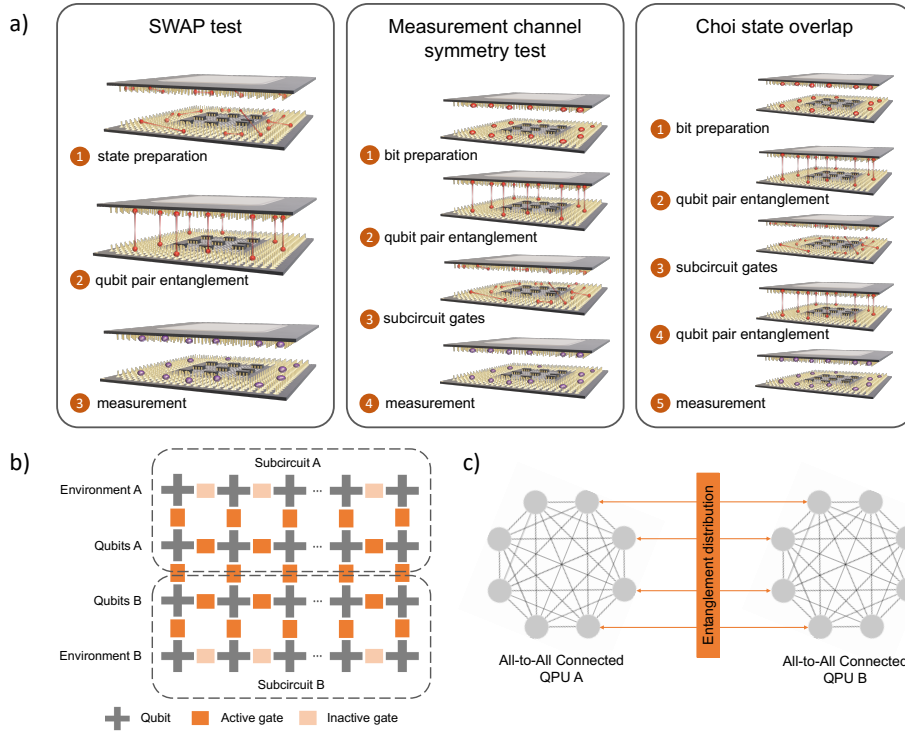


Figure 11: Examples of the compatibility of symmetry testing quantum algorithms with quantum processing units (QPUs) of variable connectivity. a) The two subcircuit abstraction of the developed algorithms and their implementation steps. The top chip represents subcircuit A and the bottom the subcircuit B. b) A two-dimensional array of qubits can explore symmetries in open quantum systems using a one-dimensional chain of nearest-neighbor interactions. c) Two all-to-all connected QPUs with pre-entangled system qubits in an event-ready scheme can explore symmetries of measurements for arbitrary qubit interactions.

Some of the existing monolithic quantum processors can be used to efficiently implement symmetry testing of open quantum systems in one-dimensional chain Hamiltonians, which are zoned into subcircuits A and B, as shown in Figure 11b. Here, the nearest-neighbor connectivity can be supported by the Google Sycamore superconducting architecture [2], while the beyond-the-nearest-neighbor interaction and multi-qubit interactions can be implemented using QuEra Aquila [76] and recent neutral atom quantum hardware advances [20], respectively.

For testing models with higher connectivity, all-to-all connected QPUs, like those offered by IonQ [56] and Quantinuum [63] trapped ion hardware or by solid state spin-qubit systems [5], can provide more versatility. Since qubits in these systems can generate spin-photon entanglement, multiple QPUs can be connected via photon-mediated entanglement distribution and double the model size in the symmetry testing algorithms (Figure 11c). Here, the success of the entanglement distribution is statistical and can be utilized in the event-ready scheme, a frequently employed approach introduced in [77] where photons originating from separate entangling processes in non-local systems become entangled on a beam-splitter and their quantum state projected in a photon-detection process. Obtaining the desired quantum state in the measurement usually takes multiple attempts, and further processing takes place only upon its confirmation when pairs of qubits in separate systems are projected onto desired Bell states. This process is suitable for implementation of the measurement symmetry test (Figure 11a) which requires entanglement between subcircuits A and B only at the beginning of the algorithm. To be able to expand this two-QPU implementation from measurement symmetry testing to the state, channel, and Lindbladian symmetry testing, additional work is needed to adapt the protocol to non-deterministic Bell measurements.

Acknowledgements—We acknowledge helpful discussions with Damien Bowen, Soorya Rethinasamy, and Hanna Westerheim. MR acknowledges support by the National Science Foundation (CAREER award No. 2047564) and the Noyce Initiative. MMW acknowledges support from the National Science Foundation under Grant No. 2315398.

References

- [1] Yakir Aharonov and Leonard Susskind. Charge superselection rule. *Physical Review*, 155(5):1428–1431, March 1967.

- [2] Frank Arute, Kunal Arya, Ryan Babbush, Dave Bacon, Joseph C. Bardin, Rami Barends, Rupak Biswas, Sergio Boixo, Fernando G. S. L. Brandao, David A. Buell, et al. Quantum supremacy using a programmable superconducting processor. *Nature*, 574(7779):505–510, 2019.
- [3] Stephen D. Bartlett, Terry Rudolph, and Robert W. Spekkens. Reference frames, superselection rules, and quantum information. *Reviews of Modern Physics*, 79(2):555–609, April 2007. arXiv:quant-ph/0610030.
- [4] Kishor Bharti, Alba Cervera-Lierta, Thi Ha Kyaw, Tobias Haug, Sumner Alperin-Lea, Abhinav Anand, Matthias Degroote, Hermanni Heimonen, Jakob S. Kottmann, Tim Menke, Wai-Keong Mok, Sukin Sim, Leong-Chuan Kwek, and Alán Aspuru-Guzik. Noisy intermediate-scale quantum (NISQ) algorithms. *Reviews of Modern Physics*, 94(1):015004, February 2022. arXiv:2101.08448.
- [5] Conor E. Bradley, Joe Randall, Mohamed H. Aboeib, R. C. Berrevoets, M. J. Degen, Michiel A. Bakker, Matthew Markham, D. J. Twitchen, and Tim H. Taminiau. A ten-qubit solid-state spin register with quantum memory up to one minute. *Physical Review X*, 9(3):031045, 2019.
- [6] Todd A. Brun. Measuring polynomial functions of states. *Quantum Information and Computation*, 4(5):401–408, September 2004. arXiv:quant-ph/0401067.
- [7] G. Cassinelli, E. De Vito, and A. Toigo. Positive operator valued measures covariant with respect to an irreducible representation. *Journal of Mathematical Physics*, 44(10):4768–4775, 2003. arXiv:quant-ph/0302187.
- [8] M. Cerezo, Andrew Arrasmith, Ryan Babbush, Simon C. Benjamin, Suguru Endo, Keisuke Fujii, Jarrod R. McClean, Kosuke Mitarai, Xiao Yuan, Lukasz Cincio, and Patrick J. Coles. Variational quantum algorithms. *Nature Reviews Physics*, 3:625–644, September 2021. arXiv:2012.09265.
- [9] Andrew M. Childs and Tongyang Li. Efficient simulation of sparse Markovian quantum dynamics. *Quantum Information and Computation*, 17(11&12):901–947, November 2016.
- [10] Andrew M. Childs and Tongyang Li. Efficient simulation of sparse Markovian quantum dynamics, 2023. arXiv:1611.05543v3.
- [11] Giulio Chiribella and Giacomo Mauro D’Ariano. Extremal covariant positive operator valued measures. *Journal of Mathematical Physics*, 45(12):4435–4447, 2004. arXiv:quant-ph/0406237.
- [12] D. Chruscinski and A. Kossakowski. Quantum entanglement and symmetry. *Journal of Physics: Conference Series*, 87(1):012008, November 2007.
- [13] Richard Cleve and Chunhao Wang. Efficient quantum algorithms for simulating Lindblad evolution. In Ioannis Chatzigiannakis, Piotr Indyk, Fabian Kuhn,

- and Anca Muscholl, editors, *44th International Colloquium on Automata, Languages, and Programming (ICALP 2017)*, volume 80 of *Leibniz International Proceedings in Informatics (LIPIcs)*, pages 17:1–17:14, Dagstuhl, Germany, 2017. Schloss Dagstuhl–Leibniz-Zentrum fuer Informatik.
- [14] E. Davies. Information and quantum measurement. *IEEE Transactions on Information Theory*, 24(5):596–599, 1978.
 - [15] Thomas Decker, Dominik Janzing, and Martin Rötteler. Implementation of group-covariant positive operator valued measures by orthogonal measurements. *Journal of Mathematical Physics*, 46(1):012104, 2005. arXiv:quant-ph/0407054.
 - [16] Andrew C. Doherty, Pablo A. Parrilo, and Federico M. Spedalieri. Distinguishing separable and entangled states. *Physical Review Letters*, 88(18):187904, April 2002. arXiv:quant-ph/0112007.
 - [17] Andrew C. Doherty, Pablo A. Parrilo, and Federico M. Spedalieri. Complete family of separability criteria. *Physical Review A*, 69(2):022308, February 2004. arXiv:quant-ph/0308032.
 - [18] Andrew C. Doherty, Pablo A. Parrilo, and Federico M. Spedalieri. Detecting multipartite entanglement. *Physical Review A*, 71(3):032333, March 2005. arXiv:quant-ph/0407143.
 - [19] T. Eggeling and R. F. Werner. Separability properties of tripartite states with $U \otimes U \otimes U$ symmetry. *Physical Review A*, 63(4):042111, March 2001.
 - [20] Simon J. Evered, Dolev Bluvstein, Marcin Kalinowski, Sepehr Ebadi, Tom Manovitz, Hengyun Zhou, Sophie H. Li, Alexandra A. Geim, Tout T. Wang, Nishad Maskara, et al. High-fidelity parallel entangling gates on a neutral atom quantum computer. arXiv:2304.05420, 2023.
 - [21] Nic Ezzell, Elliott M. Ball, Aliza U. Siddiqui, Mark M. Wilde, Andrew T. Sornborger, Patrick J. Coles, and Zoë Holmes. Quantum mixed state compiling. *Quantum Science and Technology*, 8(3):035001, April 2023.
 - [22] Ugo Fano and A. Ravi P. Rau. *Symmetries in Quantum Physics*. Academic Press, 1996.
 - [23] Jay Gambetta. Expanding the IBM quantum roadmap to anticipate the future of quantum-centric supercomputing. *IBM Research Blog*, May 2022. <https://research.ibm.com/blog/ibm-quantum-roadmap-2025>.
 - [24] Juan Carlos Garcia-Escartin and Pedro Chamorro-Posada. SWAP test and Hong-Ou-Mandel effect are equivalent. *Physical Review A*, 87(5):052330, May 2013. arXiv:1303.6814.
 - [25] Christopher Gerry and Peter Knight. *Introductory Quantum Optics*. Cambridge University Press, November 2004.

- [26] Gilad Gour and Robert W. Spekkens. The resource theory of quantum reference frames: manipulations and monotones. *New Journal of Physics*, 10:033023, March 2008. arXiv:0711.0043.
- [27] David J. Gross. The role of symmetry in fundamental physics. *Proceedings of the National Academy of Sciences*, 93(25):14256–14259, December 1996.
- [28] Masahito Hayashi. *Quantum Information Theory: Mathematical Foundation*. Springer, second edition, 2017.
- [29] Wassily Hoeffding. Probability inequalities for sums of bounded random variables. *Journal of the American Statistical Association*, 58(301):13–30, March 1963.
- [30] Alexander S. Holevo. A note on covariant dynamical semigroups. *Reports on Mathematical Physics*, 32(2):211–216, 1993.
- [31] Alexander S. Holevo. Covariant quantum dynamical semigroups: unbounded generators. In *Irreversibility and Causality Semigroups and Rigged Hilbert Spaces: A Selection of Articles Presented at the 21st International Colloquium on Group Theoretical Methods in Physics (ICGTMP) at Goslar, Germany, July 16–21, 1996*, pages 67–81. Springer, 1996.
- [32] Alexander S. Holevo. Covariant quantum Markovian evolutions. *Journal of Mathematical Physics*, 37(4):1812–1832, April 1996.
- [33] Alexander S. Holevo. Remarks on the classical capacity of quantum channel. arXiv:quant-ph/0212025, December 2002.
- [34] Alexander S. Holevo. *Probabilistic and Statistical Aspects of Quantum Theory*, volume 1. Springer Science & Business Media, 2011.
- [35] Alexander S. Holevo. *Quantum Systems, Channels, Information: A Mathematical Introduction*. de Gruyter, second edition, 2019.
- [36] Hirsh Kamakari, Shi-Ning Sun, Mario Motta, and Austin J. Minnich. Digital quantum simulation of open quantum systems using quantum imaginary–time evolution. *PRX Quantum*, 3(1):010320, February 2022.
- [37] Sumeet Khatri and Mark M. Wilde. Principles of quantum communication theory: A modern approach, 2020. arXiv:2011.04672v1.
- [38] Hari Krovi, Saikat Guha, Zachary Dutton, and Marcus P. da Silva. Optimal measurements for symmetric quantum states with applications to optical communication. *Physical Review A*, 92:062333, December 2015. arXiv:1507.04737.
- [39] Margarite L. LaBorde. *A Menagerie of Symmetry Testing Quantum Algorithms*. PhD thesis, Louisiana State University, Department of Physics and Astronomy, 2023. arXiv:2305.14560.
- [40] Margarite L. LaBorde, Soorya Rethinasamy, and Mark M. Wilde. Testing symmetry on quantum computers. arXiv:2105.12758, May 2021.

- [41] Margarite L. LaBorde, Soorya Rethinasamy, and Mark M. Wilde. Quantum computational complexity and symmetry. In preparation, 2023.
- [42] Margarite L. LaBorde and Mark M. Wilde. Quantum algorithms for testing Hamiltonian symmetry. *Physical Review Letters*, 129(16):160503, October 2022.
- [43] Martín Larocca, Frédéric Sauvage, Faris M. Sbahi, Guillaume Verdon, Patrick J. Coles, and M. Cerezo. Group-invariant quantum machine learning. *PRX Quantum*, 3(3):030341, September 2022.
- [44] Felix Leditzky, Eneet Kaur, Nilanjana Datta, and Mark M. Wilde. Approaches for approximate additivity of the Holevo information of quantum channels. *Physical Review A*, 97(1):012332, January 2018.
- [45] Elliott H. Lieb and Robert Seiringer. *The Stability of Matter in Quantum Mechanics*. Cambridge University Press, Cambridge, UK, December 2009.
- [46] Göran Lindblad. Completely positive maps and entropy inequalities. *Communications in Mathematical Physics*, 40(2):147–151, June 1975.
- [47] Göran Lindblad. On the generators of quantum dynamical semigroups. *Communications in Mathematical Physics*, 48(2):119–130, June 1976.
- [48] Matteo Lostaglio, Kamil Korzekwa, David Jennings, and Terry Rudolph. Quantum coherence, time-translation symmetry, and thermodynamics. *Physical Review X*, 5(2):021001, April 2015.
- [49] Jonathan Z. Lu, Rodrigo A. Bravo, Kaiying Hou, Gebremedhin A. Dagnaw, Susanne F. Yelin, and Khadijeh Najafi. Learning quantum symmetries with interactive quantum-classical variational algorithms. arXiv:2206.11970, 2023.
- [50] Iman Marvian. *Symmetry, asymmetry and quantum information*. PhD thesis, University of Waterloo, September 2012. <http://hdl.handle.net/10012/7088>.
- [51] Iman Marvian and Robert W. Spekkens. The theory of manipulations of pure state asymmetry: I. basic tools, equivalence classes and single copy transformations. *New Journal of Physics*, 15(3):033001, March 2013. arXiv:1104.0018.
- [52] Iman Marvian and Robert W. Spekkens. Modes of asymmetry: The application of harmonic analysis to symmetric quantum dynamics and quantum reference frames. *Physical Review A*, 90(6):062110, December 2014. arXiv:1312.0680.
- [53] Iman Marvian and Robert W. Spekkens. How to quantify coherence: Distinguishing speakable and unspeakable notions. *Physical Review A*, 94(5):052324, November 2016.
- [54] Johannes Jakob Meyer, Marian Mularski, Elies Gil-Fuster, Antonio Anna Mele, Francesco Arzani, Alissa Wilms, and Jens Eisert. Exploiting symmetry in variational quantum machine learning. *PRX Quantum*, 4(1):010328, March 2023.

- [55] Alexander Miessen, Pauline J. Ollitrault, Francesco Tacchino, and Ivano Tavernelli. Quantum algorithms for quantum dynamics. *Nature Computational Science*, 3(1):25–37, December 2022.
- [56] Christopher Monroe. IonQ quantum computers: clear to scale. In *APS March Meeting Abstracts*, volume 2021, pages P10–002, 2021.
- [57] Masanao Ozawa. Entanglement measures and the Hilbert–Schmidt distance. *Physics Letters A*, 268(3):158–160, April 2000. arXiv:quant-ph/0002036.
- [58] David Pérez-García, Michael M. Wolf, Denes Petz, and Mary Beth Ruskai. Contractivity of positive and trace-preserving maps under L_p norms. *Journal of Mathematical Physics*, 47(8):083506, August 2006. arXiv:math-ph/0601063.
- [59] Soorya Rethinasamy, Rochisha Agarwal, Kunal Sharma, and Mark M. Wilde. Estimating distinguishability measures on quantum computers. *Physical Review A*, 108(1):012409, July 2023. arXiv:2108.08406.
- [60] Anthony W. Schlingens, Kade Head-Marsden, LeeAnn M. Sager, Prineha Narang, and David A. Mazziotti. Quantum simulation of the Lindblad equation using a unitary decomposition of operators. *Physical Review Research*, 4(2):023216, June 2022.
- [61] Andrea Skolik, Michele Cattelan, Sheir Yarkoni, Thomas Bäck, and Vedran Dunjko. Equivariant quantum circuits for learning on weighted graphs. *npj Quantum Information*, 9(1):47, May 2023.
- [62] Alexander Streltsov, Gerardo Adesso, and Martin B. Plenio. Colloquium: Quantum coherence as a resource. *Reviews of Modern Physics*, 89(4):041003, October 2017.
- [63] Russell Stutz. Trapped ion quantum computing at Quantinuum. In *APS March Meeting Abstracts*, volume 2022, pages M28–005, 2022.
- [64] Yiğit Subaşı, Lukasz Cincio, and Patrick J. Coles. Entanglement spectroscopy with a depth-two quantum circuit. *Journal of Physics A: Mathematical and Theoretical*, 52(4):044001, January 2019. arXiv:1806.08863.
- [65] Nishchay Suri, Joseph Barreto, Stuart Hadfield, Nathan Wiebe, Filip Wudarski, and Jeffrey Marshall. Two-unitary decomposition algorithm and open quantum system simulation. *Quantum*, 7:1002, May 2023.
- [66] Matthew Treinish et al. Qiskit: An open-source framework for quantum computing, 2023. <https://doi.org/10.5281/zenodo.2573505>.
- [67] Géza Tóth and Iagoba Apellaniz. Quantum metrology from a quantum information science perspective. *Journal of Physics A: Mathematical and Theoretical*, 47(42):424006, October 2014.
- [68] Armin Uhlmann. The “transition probability” in the state space of a *-algebra. *Reports on Mathematical Physics*, 9(2):273–279, April 1976.

- [69] Thomas Vidick and John Watrous. Quantum proofs. *Foundations and Trends in Theoretical Computer Science*, 11(1–2):1–215, March 2016. arXiv:1610.01664.
- [70] John Watrous. Limits on the power of quantum statistical zero-knowledge. *Proceedings of the 43rd Annual IEEE Symposium on Foundations of Computer Science*, pages 459–468, November 2002. arXiv:quant-ph/0202111.
- [71] John Watrous. Quantum computational complexity. *Encyclopedia of Complexity and System Science*, 2009. arXiv:0804.3401.
- [72] John Watrous. *The Theory of Quantum Information*. Cambridge University Press, Cambridge, 2018.
- [73] Reinhard F. Werner. An application of Bell’s inequalities to a quantum state extension problem. *Letters in Mathematical Physics*, 17(4):359–363, May 1989.
- [74] G. C. Wick, A. S. Wightman, and E. P. Wigner. The intrinsic parity of elementary particles. *Physical Review*, 88(1):101–105, October 1952.
- [75] Mark M. Wilde. *Quantum Information Theory*. Cambridge University Press, Cambridge, UK, second edition, 2017.
- [76] Jonathan Wurtz, Alexei Bylinskii, Boris Braverman, Jesse Amato-Grill, Sergio H. Cantu, Florian Huber, Alexander Lukin, Fangli Liu, Phillip Weinberg, John Long, et al. Aquila: Quera’s 256-qubit neutral-atom quantum computer. arXiv:2306.11727, 2023.
- [77] Bernard Yurke and David Stoler. Bell’s-inequality experiments using independent-particle sources. *Physical Review A*, 46(5):2229, 1992.